Remote Sensing of Environment 318 (2025) 114545

Contents lists available at ScienceDirect

Remote Sensing of Environment

journal homepage: www.elsevier.com/locate/rse

# LiDAR-derived Lorenz-entropy metric for vertical structural complexity: A comparative study of tropical dry and moist forests

Nooshin Mashhadi [a], Arturo Sanchez-Azofeifa [a,*], Ruben Valbuena [b]

[a] Department of Earth and Atmospheric Sciences, Centre for Earth Observation Sciences, University of Alberta, T6G 2E3 Edmonton, Canada
[b] Department of Forest Resource Management, Swedish University of Agricultural Sciences, Umeå, Sweden

ARTICLE INFO

Edited by Jing M. Chen

*Keywords:*
Entropy
Structural complexity
Structural diversity
LiDAR
Biodiversity
Evenness

ABSTRACT

This study introduces an Entropy-based index: the Lorenz-entropy (LE) index, which we have developed by integrating Light Detection And Ranging (LiDAR), econometrics, and forest ecology. The main goal of the LE is to bridge the gap between theoretical entropy concepts and their practical applications in monitoring vertical structural complexity of tropical forest ecosystems. The LE index quantifies entropy by analyzing Relative Height (RH) metrics (representing a one-dimensional (1D) canopy structure metric) distributions from full-waveform LiDAR across successional stages in a tropical dry forest (TDF) and a tropical rainforest. To validate the LE trends derived from LiDAR, we extended the analysis using inventory-based two-dimensional (2D) and three-dimensional (3D) metrics, specifically basal area and biomass. The consistency of trends between the 1D LiDAR-derived LE and the inventory-based 2D and 3D metrics reinforces the LE's ability to capture and monitor structural complexity reliably across different measurement dimensions.

Our findings demonstrated that LE captures the changes in entropy as a function of successional stages, reflecting how canopy structure evolves towards homogeneity and complexity. Our statistical analysis revealed significant differences between successional stages (ANOVA, $\alpha = 0.05$, $p <$ 2e-16), with LE increasing substantially from early to late stages and plateauing at climax, where vertical structure (entropy) stabilizes. The mean LE increased by $1.70\times10^{-2}$ between late and climax stages, with a small effect size (Cohen's d = 0.25), indicating minor differences in complexity. The LE index, calculated from biomass and basal area, confirming that as forests mature, entropy and vertical structural complexity increase. Furthermore, the sensitivity analysis showed that LE is most responsive to RHs variability during intermediate stages, suggesting that structural development is most dynamic during this phase. These results demonstrate the potential of the LE index as a tool for ecological analysis and monitoring forest dynamics.

## 1. Introduction

Describing forest ecological characteristics requires an approach that takes into consideration the inter- and intra-relationships that exist between crucial ecosystem variables, such as species diversity, richness, abundance, complexity, biomass, and productivity (Vranken et al., 2015; Harte et al., 2022). Several studies have shown that estimating ecosystem variables (e.q. nutrient cycling, energy flow, and species abundance) requires consideration of interconnections among them (De Boeck et al., 2020; Geary et al., 2020). On the other hand, the more structurally complex the habitat, the greater the species diversity and richness (Kohn and Leviten, 1976; St. Pierre and Kovalenko, 2014; Malhi et al., 2022). Habitats with high structural complexity often have multiple layers of vegetation, such as canopies, understories, and ground cover and a greater diversity of microhabitats and niches, which can support a wider range of species (Edeline et al., 2023). This layered structure allows for more efficient capture and use of sunlight, increasing overall photosynthetic productivity (Coverdale and Davies, 2023). Higher photosynthetic productivity means more energy is available at the base of the food web (Cushman, 2023). This energy supports a larger and more diverse array of herbivores, which supports greater diversity (Ray et al., 2023). This suggests a strong link between habitat complexity and photosynthetic productivity, that manifest across different spatial and temporal scales (Malhi et al., 2015; Harte et al., 2022; Cushman, 2023). The relationships between complexity, biodiversity, and productivity provide valuable insights into the

* Corresponding author.
*E-mail address:* arturo.sanchez@ualberta.ca (A. Sanchez-Azofeifa).

https://doi.org/10.1016/j.rse.2024.114545
Received 29 May 2024; Received in revised form 27 November 2024; Accepted 27 November 2024
Available online 6 December 2024

ecosystem (Cushman, 2015; Brun et al., 2019). Therefore, having a reliable indicator that can reflect all these significant variables is necessary.

### 1.1. Entropy in forest ecology

Scientists have been facing the challenge of finding a universal law that can be applied to forest ecology and natural sciences (Lawton, 1999; Duchesne et al., 2001; Li et al., 2004). To address this lack of understanding, since Vranken et al. (2015), significant advancements have been made in this area, driven by new technologies and methodologies. These include advanced remote sensing technologies, such as Light Detection and Ranging (LiDAR) and hyperspectral imaging, have provided high-resolution data on forest structure (Gandharum et al., 2022; Liesenberg, 2022). These tools have enabled detailed analyses of canopy height, biomass, and spatial complexity, offering new insights into forest dynamics (Liu et al., 2022). Moreover, research on functional diversity has progressed significantly. New methods for quantifying functional traits and linking them to ecosystem processes have improved our understanding of how biodiversity influences productivity, resilience, and nutrient cycling (Huxley et al., 2023; Yan et al., 2023a). In addition, advances in ecosystem modeling have enhanced our ability to predict forest responses to environmental changes. These models incorporate structural complexity, species interactions, and climatic variables, providing more accurate predictions of forest dynamics and productivity (Papastefanou et al., 2023).

Clausius, in 1850, established Entropy as a system state function, rooting it in classical thermodynamics. Initially, its purpose was to measure the extent of irreversibility in a thermodynamic transformation within an isolated system (Li et al., 2004). Subsequently, entropy had numerous interpretations and applications, notably paralleling developments in information theory. Claude Shannon (1948) developed an alternative use for the term. This alternative approach contrasted with the thermodynamic perspective, which focuses on systems operating "far from equilibrium" (Nielsen et al., 2020). Shannon's information theory examines entropy in relation to the disorder present in nature. In landscape ecology, researchers use entropy as a descriptor of patterns or processes, referencing thermodynamics to varying extents (Vranken et al., 2015).

Various indices examine species diversity in ecological communities (Zaccarelli et al., 2013) (Supplementary Table 1). These indices aim to estimate uncertainties in their relative abundance (Jost, 2006). As such, it can be deduced that the maximum level of uncertainty (entropy) occurs at the highest level (Zaccarelli et al., 2013; Cushman, 2021, 2023). In a pioneering study using entropy-based indices in ecology, Macarthur and Macarthur (1961) conducted a significant study using Shannon entropy (Shannon, 1948) to examine species diversity in ecological communities and in forests based on variations in tree size. This index is known as Foliage Height Diversity (FHD) (Macarthur and Macarthur, 1961; Valbuena et al., 2012). The FHD assumes that the canopy vertical structure is divided into different foliage layers within a canopy in which the FHD is highly dependent on the number and size of these layers or bins, although it is unusual for describing continuous variables, such as canopy height (Valbuena et al., 2021). Moreover, entropy-based metrics became tools for measuring diversities within ecosystems in ecological research, encompassing both species diversity, such as the Shannon-Weiner diversity index, and landscape diversity, exemplified by the contagion index (Hill, 1973; Li and Reynolds, 1993; Vranken et al., 2015).

Cushman (2018) has demonstrated that an irreversible increase in entropy, resulting from interactions among forest components, reduces free energy. As a result, Cushman's (2018) theory provides the basis for estimating biodiversity at different scales of structural (Alpha, Beta, and Gamma) (Orlóci, 1991; Meffe et al., 2002) as well as functional diversity (functional traits of species complexity (Cadotte, 2017; Mason et al., 2005)).

### 1.2. Gini coefficient and Lorenz curve

The Gini coefficient (GC) is an econometric variable used to quantify inequality, that is employed in several fields, including forest ecology (Weiner and Solbrig, 1984; Weiner et al., 1990; Valbuena et al., 2016; Valbuena et al., 2021). It was first established by Corrado Gini (Gini, 1912, 1921) and later derived from the Lorenz curve by Max Otto Lorenz (Lorenz, 1905) (Fig. 1). Research conducted by Lexerød and Eid (2006) proposing the GC indicator as a tool, contributed to the understanding of structural diversity and complexity in forests. Moreover, Valbuena et al. (2013a) utilized the GC due to its robustness and reliability in representing size distribution and heterogeneity within forest stands. Their results were validated through high-accuracy airborne laser scanning data, ensuring the precision of the derived forest structural metrics. They also demonstrated that using the GC is particularly significant when compared to other indicators like the coefficient of variation or skewness, which may be influenced by sample size and distribution shape. This indicator scrutinizes the interrelations of relative dominance within forest assemblages and can be employed to compare the heterogeneity between distinct forest stands within a chronosequence (Weiner and Solbrig, 1984; Weiner et al., 1990). Valbuena et al. (2016) demonstrated the mathematical basis of the GC includes the assumption that forest metrics, such as tree heights, are continuous variables, which is essential for accurately calculating the statistical dispersion using the GC. Furthermore, the input measurements must be positive to maintain data integrity during the coefficient's computation. The GC also necessitates ordinal consistency, meaning the values must be ordinal and can be meaningfully ranked. Additionally, the values must be summable, summing to a finite number, allowing the GC to be normalized and constrained between 0 and 1. To prevent estimation bias, each data point must be independent. Lastly, the finite population size assumption is a practical consideration for computing the GC, ensuring its applicability and reliability in empirical research.

Linkages between the Lorenz curve and forest structure have also been studied; for instance, Damgaard and Weiner (2000) found that the Lorenz curve can be effectively utilized to interpret the composition of vertical strata in a forest. Later, Adnan et al. (2021) as well as Valbuena et al. (2021) found that the maximum entropy in a Lorenz curve (henceforth referred to as *MAXENT(GC)*) can be determined according

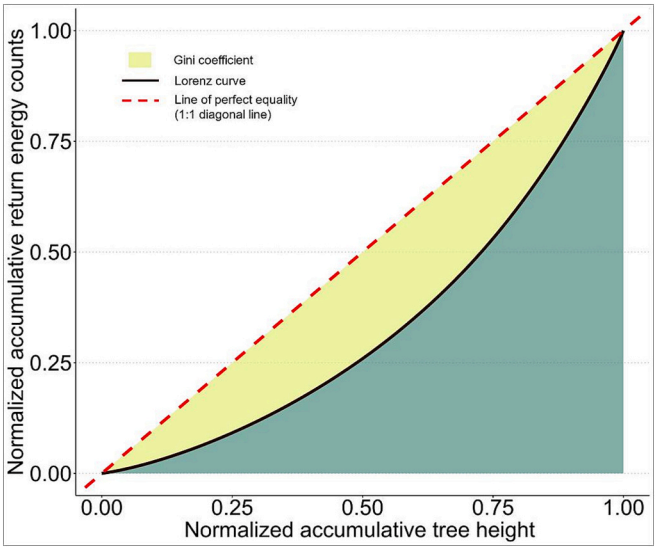


**Fig. 1.** Theoretical calculation of the Gini coefficient from airborne LiDAR data. The solid line is the Lorenz curve, while the area between the Lorenz curve and the red diagonal dashed line (also known as the line of perfect equality) is the Gini coefficient. (For interpretation of the references to colour in this figure legend, the reader is referred to the web version of this article.)

to the dimensionality of the variable used to assess the ecosystem, whether using height ($GC_H$; unidimensional = 0.33), basal area ($GC_{BA}$; bidimensional = 0.50), or Above Ground Biomass (AGB) ($GC_{AGB}$; tridimensional = 0.60) (Valbuena et al., 2021). From this research it arises that an entropy-focused index that substitutes FHD (section 1.1) is still needed, and possible to be constructed from the GC as discussed in Valbuena et al. (2021) early work.

In quantifying forest structure, measuring complexity allows for evaluating the integrity and resilience of complex environmental systems (Ehbrecht et al., 2021). The complexity and variety of structural components in an ecosystem usually directly relate to the level of biodiversity (Gamfeldt and Roger, 2017; Heidrich et al., 2020). Structural complexity involves the interaction between various attributes and variables, challenging quantitative comparisons between stands (Spies and Franklin, 1991). Hence, several indices have been created to address this issue and express structural complexity as a singular number (Newsome and Catling, 1979; Koop et al., 1995). These indices serve as concise representations of various structural attributes and can be used to rank forest stands based on their potential impact on biodiversity (Van et al., 2000; Parkes et al., 2003). For example, Zenner (2000) derived a Structural Complexity Index (SCI) from a three-dimensional forest structure model that was linked to the standard deviation of Diameter at Breast Height (DBH). Additionally, Neumann and Starlinger (2001) determined that the standard deviation of DBH was significantly correlated with the seven structural complexity indices (Pielou index, Cox index, Clark-Evans index, Gadow index, Vertical evenness index, Holdridge complexity index, and Stand Diversity index) examined.

Among forest biomes, tropical forest ecosystems are known for their remarkable structural complexity and high biodiversity, which Ehbrecht et al. (2021) attributed these characteristics primarily to environmental factors such as climate and soils. The structural complexity of tropical forests arises from the interplay between the various functional traits of plant species (Faccion et al., 2021; Coverdale and Davies, 2023; Mitchell et al., 2023). These traits include tree height, crown architecture, leaf size and shape, root systems, and reproductive strategies. Different species possess distinct combinations of these traits, contributing to forest structure's vertical and horizontal heterogeneity.

To date, several studies have demonstrated methods for calculating entropy, diversity, and complexity (Bertram, 2014; Wang and Zhao, 2018; Cushman, 2021; Pos et al., 2023). A common limitation of these studies is the lack of use of emerging technologies, such as airborne or spaceborne Light Detection and Ranging (LiDAR) data, to describe the structural diversity and complexity of forest ecosystems in the context of entropy. Recently, Liu et al. (2022) proposed an entropy-based canopy structural complexity index using Terrestrial Laser Scanning (TLS), backpack laser scanning, and Unmanned Aerial Vehicle Laser Scanning (ULS). While these methodologies have proven effective, they have limitations regarding, data fusion challenges, and generalizability issues. Although traditional diversity indices, such as species counts and the Shannon and Simpson indices (Hill, 1973; Magurran, 2004; Morris et al., 2014; Konopiński, 2020), have been used to represent species diversity and complexity, measuring these indices in the field is often impractical. Moreover, some important structural aspects such as the vertical arrangement of trees, the distribution of gaps in the canopy, and canopy layering are harder to assess in the field. As the level of detail in the field inventory increases, the area that can be covered by the inventory decreases (Atkins et al., 2023). This highlights the need for a method to measure the vertical structural complexity using remote sensing technology such as airborne LiDAR, across different scales.

### 1.3. Objective

In this paper, we aim to develop a new entropy-based indicator called the Lorenz-entropy (LE) index, which is built upon the Gini Coefficient (GC) measurements of variability in the Lorenz curve (Valbuena et al., 2016). The GC quantifies the inequality in the distribution of a variable, such as canopy height, by providing a single value that represents this inequality. In contrast, the LE index expands on this concept by incorporating entropy, which measures the complexity and disorder within the distribution. This integration allows the LE index to capture the forest ecosystem's inequality and vertical structural complexity. The LE is based on a mathematical framework developed by Valbuena et al. (2021) for assessing LiDAR-based entropy in tropical forest ecosystems. The LE index can be considered an ecological analog that integrates thermodynamics, information theory, remote sensing, and econometrics. We employed the *MAXENT(GC)* from the study by Adnan et al. (2021) to develop the LE index at the footprint level using unidimensional airborne LiDAR metrics, Relative Heights (RHs, $GC_H$; unidimensional = 0.33). Additionally, we employed two-dimensional (Basal Area) and three-dimensional (Above Ground Biomass - AGB) tree metrics to validate the outcomes derived from this index. The focus of our study is to ascertain the applicability of the LE index in quantifying entropy across two distinct types of tropical forest ecosystems, a tropical dry forest under different stages of ecological succession, and a tropical rainforest on the climax stage.

## 2. Methods

### 2.1. Conceptual foundation for the development of a Lorenz-entropy index

The conceptual model, developed for this study representing in Fig. 2. In this figure, the LE metric is located along the vertical axis. In contrast, the horizontal axis displays the range of the GC values, indicating the level of inequality in the ecosystem. The LE trajectory can rise from left to right (trajectory a) or right to left (trajectory b) based on Janzen's (1988) tropical generation theory, reaching a maximum value of one at the highest point of maturity and entropy (trajectory c, Adnan et al., 2021).

$$\text{Trajectory a} : \text{GC} \in ]0, 0.33[.$$

$$\text{Trajectory b} : \text{GC} \in ]0.33, 1[.$$

$$\text{Trajectory c} : \text{GC} = 0.33.$$

On the left side of this diagram, LE increases from a GC of zero to 0.33. This point (GC = 0) indicates a tropical ecosystem that originates from complete uniformity, for instance, pastureland. The example waveform shows a vertical structure representing each chronosequence stage (detailed information is explained in section 2.4). From the waveform in the early stage of the left side, the uniformity of the distribution of trees is visible. A different scenario is presented on the right side of the diagram. Starting from a GC = 1, this scenario of forest regeneration begins with a single tree species, known as a nuclear tree; as it is represented in its early stage waveform, it can be interpreted that there is a rise in amplitude before the ground level (Elevation =0). Then, the ecosystem gradually expands to the next ecological succession stage (Janzen, 1988). After the ecosystem expanded, canopy height became relatively homogenous, with no significant variation in tree height. Moreover, on this side (left side of the diagram), the ecosystem transitions from a state of low structural diversity to a state of high uniformity, and it experiences a significant reduction in the GC, which reaches a final equilibrium value of 0.33. The same scenario is adhered to by employing basal area and tree volume as bi-dimensional and three-dimensional forest metrics. These metrics represent different aspects of forest structure, and the complexity captured by them varies with their dimensionality, necessitating adjustments to the MAXENTGC to account for these differences. This approach allows for meaningful comparisons between different types of forest structural measurements and ensures that entropy values are accurately scaled and comparable across various types of measurements, enhancing the robustness and

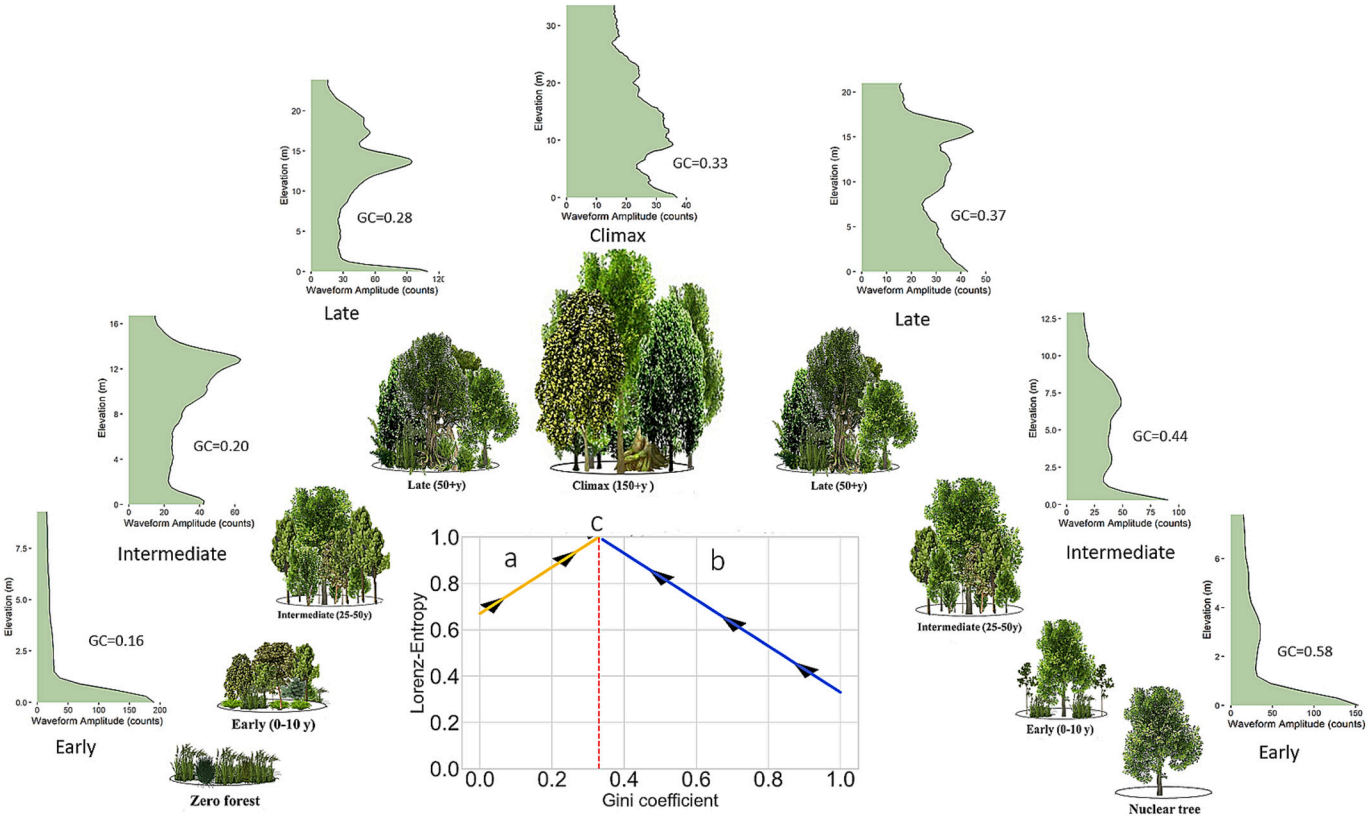


**Fig. 2.** The Gini coefficient vs. Lorenz-entropy (LE). The red dashed line is the maximum entropy of the Gini coefficient (GC = 0.33 for one-dimensional variable). The arrows representing the trajectory direction of the LE from the left side (yellow colour) a:]0,0.33[, and right side (blue colour) b:]0.33,1[towards the maximum value. The waveform represents the sample waveform for early, intermediate, and late successional stages for each different trajectories towards the climax stage with their corresponding GC. Differences between each side of the trend in the forest ecosystems are represented by the successional stages as defined by Arroyo Mora et al. (2005). (For interpretation of the references to colour in this figure legend, the reader is referred to the web version of this article.)

accuracy of the Lorenz-entropy (LE) index.

Nonetheless, it is important to note that Adnan et al. (2021), derived the maximum entropy of the GC ($MAXENT_{GC}$) for two-dimensional as and the three-dimensional tree measurements, as e 0.50, and 0.60, respectively.

### 2.2. Calculation of Lorenz-entropy (LE) index

The theoretical foundation of our method is rooted in the second principle of thermodynamics, whereby "*entropy manifests as a perpetually positive and ascending entity*" (Nielsen et al., 2020). As such our index is derived from the difference between the GC and its maximum entropy value (MAXENT) (Eq. (1)). This method considers canopy height extracted from the waveform airborne LiDAR to generate Lorenz curves and to quantify the GC. Consequently, the absolute value of the GC deviation from MAXENT(GC) is considered to maintain a positive attribute invariably (Eq. (1)).

$$LE = 1 - (|MAXENT(GC) - GC|) \quad (1)$$

Where the GC for continuous variables is calculated based on the area under the Lorenz curve derived using an airborne LiDAR system such as the Land Vegetation and Ice Sensor (LVIS) waveform data (Eq. (2), Fig. 1). After the pre-processing of LiDAR data obtained from LVIS as described in (Blair et al., 1999; Gu et al., 2018), the computation of the GC was performed.

The Lorenz curve was plotted by normalizing the cumulative canopy height against normalized cumulative energy returns. The GC was then calculated using the method proposed by Adnan et al. (2021), which involved calculating the Cumulative Distribution Function (CDF) of canopy height data using the trapezoidal rule for each footprint (Eq. (2)). During this process, the constant 1/2 and the trapezoidal rule with 0.05 interval widths were utilized (Eq. (3)). Moreover, it is important to note that the GC is a measure of inequality (Gini, 1921), and is usually sensitive to the shape of the distribution and can be influenced by the choice of bin widths (Lexerød and Eid, 2006), which can affect the visual representation of the data and the interpretation of the distribution. For this reason, the accuracy of the GC can be affected by underestimation/bias and the variance in the data. In LVIS waveform data RH0 and RH100 represent the heights at which 0 % and 100 % of the total waveform energy occurred, respectively. To create Lorenz curve and then calculate the GC the RH value between 0 and 100 was divided into the bins with range of 5 % energy interval (RH0, RH5, RH10, …, RH95, RH100). To account for a sample bias due to the binning in the estimation process, a correction factor (n/(n-1)) based on the research by Valbuena & Nabuurs (2013b), and Sitthiyot and Holasut (2021) was applied to Eq. (3), resulting a new equation (Eq. (4)). Here we considered a 5 % interval in accordance with Relative Height (RH) metrics intervals from the LVIS (Anderson et al., 2006), therefore the resulting number of bins between 0 and 100 % was 20. Thus, the correction factor used was n/(n-1) = 20/19.

$$\text{The area under the } F(y) = \sum_{i=1}^{k-1}\left(\frac{F(y_i)+F(y_{i+1})}{2}\times 0.05\right) \quad (2)$$

$$GC = ½ - \left(\sum_{i=1}^{k-1}\left(\frac{F(y_i)+F(y_{i+1})}{2}\times 0.05\right)\right) \quad (3)$$

$$GC = (n/n-1)^{*}\left[1 \Big/ 2 - \left(\sum_{i=1}^{k-1}\left(\frac{F(y_i)+F(y_{i+1})}{2}\times 0.05\right)\right)\right] \quad (4)$$

The *y* values are a set of individual canopy heights from airborne LiDAR footprint data. *F(y)* is a function of the Normalized Cumulative Height vs. the Normalized Cumulative Return of energy counts (Fig. 1), n is the Number of bins considered to create the Lorenz curve.

### 2.3. Study areas

This study was conducted in two tropical forests: i) a tropical dry forest at the Santa Rosa National Park Environmental Monitoring Supersite (SRNP-EMSS) in Costa Rica, and ii) La Selva Biological Station (Costa Rica) a wet tropical forest (Fig. 3). These two ecosystems provide different precipitation patterns, temperature, and relative humidity ranges. The SNRP-EMSS site experiences an average rainfall of 1720 mm per year. The majority of precipitation occur during the wet season from June to November with minimal water availability during the dry season from December to May (Kalácska et al., 2005). The annual average temperature is 25 °C. Vegetation in the park is classified into three successional stages based on ecosystem structure and composition: early, intermediate, and late (Kalacska et al., 2004). La Selva Biological Station (LS) tropical wet forest is in a climax stage (Hartshorn, 1980; Knight, 1975) and is located in the Atlantic lowlands of northeastern Costa Rica. The average annual rainfall at LS is 4000 mm, and the mean temperature is 26 °C. The majority of precipitation occurs during the wet season from May to January, with a minimal water availability during the dry season from February to April (Jiménez-Rodríguez et al., 2020).

### 2.4. Data curation and processing

#### 2.4.1. Data acquisition

The data used in this study was collected in March 2005 over the SRNP-EMSS and La Selva Biological Station (LS). Using the Land Vegetation Ice Sensor (LVIS) Level 1B Geolocated Waveform (.LGW) and Level 2 Ground Elevation (.LGE) (version 1.02) with a 20-m footprint. The data were obtained from the LVIS website (https://lvis.gsfc.nasa.gov/).

#### 2.4.2. Waveform LiDAR data pre-processing

The LVIS data underwent two pre-processing steps: first, the effective waveform was produced using LGW and LGE; second, the Lorenz curve was generated (Fig. 1), and the GC was calculated (Eq. (4)). Pre-processing was performed using R (version 4.1.1) and RStudio (version 2021.9.0.351).


**Fig. 3.** Study sites of tropical forests: Santa Rosa National Park Environmental Monitoring Supersite (SRNP-EMSS) in Costa Rica, and La Selva Biological Station (Costa Rica). The Santa Rosa site has different levels of ecological succession while La Selva is considered a mature tropical forest on climax.

#### 2.4.3. Calculation Gini coefficient from the waveform

A Savitzky-Golay signal processing smoothing filter was applied to the waveform data using the R package (Moreno et al., 2023), and a moving average function was used to smooth the waveform data and calculate the elevation height. A threshold function was applied to define the ground, where all values below the threshold were set to zero, allowing for elevation calculation.

The original LiDAR waveform for each LVIS footprint was generated using LGW data, which involved waveform amplitude (counts) on the x-axis and elevation on the y-axis. According to LVIS metadata, the waveform amplitude was calculated as the difference between the wave (return energy) and the sigmean, the mean signal noise level during flight. To calculate the elevation, the height between the highest sample (Z0) and lowest sample (Z431) was divided by 432, the total number of returns in each waveform.

After detecting the ground elevation (zg) and top of the canopy elevation (zt), the canopy height was calculated by subtracting zg from zt. A graph with the canopy height elevation on the y-axis and normalized cumulative return of energy (counts) on the x-axis was created for each footprint. The accumulated normalized canopy height elevation was plotted on the x-axis, and the accumulated normalized return of energy (counts) was plotted on the y-axis to create a Lorenz curve. The GC was calculated for each 20-m footprint by determining the area between the Lorenz curve and the equitability line (1:1), in accordance with Adnan et al. (2021) (Eq. (3)).

To represent the steps required for capturing the Lorenz curve to calculate the LE and the GC from the LVIS waveform data, we collected 25 sample footprints (Zhao et al., 2021) from various successional stages of the study areas, namely the early, intermediate, and late stages from the SRNP-EMSS, and the climax stage from the LS (Fig. 4).

### 2.5. Successional forest stages

In the SRNP-EMSS, forest successional stages were identified using the final map results from studies conducted by Gu et al. (2018) and Zhao et al. (2021). Their approach involved statistical analysis and image classification using LiDAR metrics, and hyperspectral images. The study calculated 21 LiDAR metrics, which were categorized into point-based, line-based, area-based, and shape-based groups derived from LiDAR waveforms and normalized cumulative return energy curves. Their results were represented on a map, showing the different areas of SRNP-EMSS assigned to early, intermediate, and late stages (Supplementary Table 4).

La Selva Biological Station (LS) is considered a mature wet forest in the climax succession. The climax stage is the mature forest, which has a regeneration of dominant tree species. However, applying this criterion is challenging due to the vast diversity of species, lack of clear dominance in most tropical forests, and taxonomic unfamiliarity (Hartshorn, 1980). The fact that a forest's dominant demographic remains stable is a strong indicator that the forest it occupies is in a state of dynamic equilibrium. In other words, it is a mature forest (Beard, 1944; Hartshorn, 1980; Feeley et al., 2011).

### 2.6. Statistical analysis

We conducted a one-way ANOVA (Analysis of variance) test to determine if the LE can effectively distinguish between the four successional stages (early, intermediate, late, and climax) and to analyze whether our hypothesis, which suggests that the LE increases from the early to late stages, then levels off at equilibrium during the climax stage, is supported. Given that the dataset for each stage comprised a

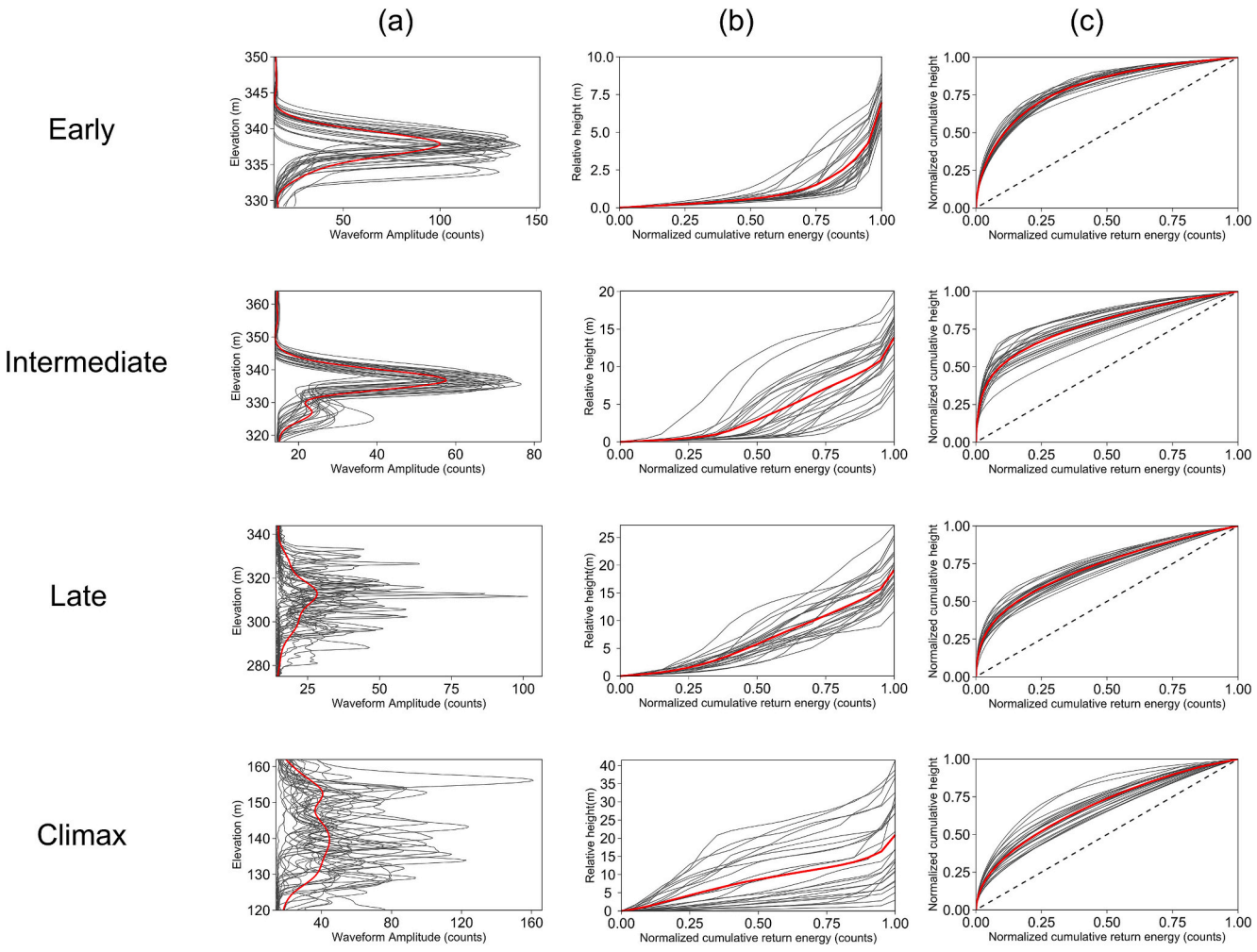


**Fig. 4.** Effective LiDAR waveform (a), normalized cumulative return energy curves (b), and Lorenz curve (c). The red line in each figure represents the average of the corresponding twenty-five curves. (For interpretation of the references to colour in this figure legend, the reader is referred to the web version of this article.)

substantial number of observations, from LVIS footprint data, the pre-requisites for ANOVA, particularly the assumptions of normality and homogeneity of variances, were deemed less stringent. This is due to the Central Limit Theorem (CLT) and the tolerance of ANOVA towards deviations from these assumptions. Prior to running the ANOVA and post hoc tests, we tested the residuals for normality using the Q-Q plot test and for heteroskedasticity using Levene's test (Levene, 1960). These tests confirmed that the assumptions of normality and homogeneity of variances were met, validating the use of ANOVA and subsequent post hoc tests for our analysis.

A one-way ANOVA allowed us to simultaneously analyze and compare the effects of the successional stages (Early, Intermediate, Late, Climax) on the two variables, the GC and the LE (Fig. 5a, and b, and details in supplementary Tables 2, and 3). Moreover, to assess the extent of change, we computed the Cohen's d values (Cohen, 1988) for each pair comparison in ANOVA.

### 2.7. Characterizing the Lorenz-entropy relative to the scale of waveform

This study calculated Lorenz-entropy (LE) using LiDAR waveforms by incorporating both the 20 m footprint size and tree distribution within each footprint. This dependency of the LE computation based on the waveform making its applicability dependent on the availability and quality of the waveform rather than the specific unit area (e.g., footprint size). Studies by Gu et al. (2018), Duan et al. (2023), and Liu et al., 2023 have explored the potential of shape-based LiDAR metrics derived from LVIS data to differentiate various successional stages in Tropical Dry Forests (TDFs). Following these studies, we analyzed the shape of each waveform (Elevation vs. Amplitude, Fig. 6) and computed three shape-based LiDAR metrics: the x-coordinate of the waveform centroid (Cx), the y-coordinate of the waveform centroid (Cy), and the radius of gyration (RG) (Table 1, Eq. (5)). These metrics were selected to capture the structural characteristics of the canopy within each 20 m footprint, providing insights into the vertical and horizontal distribution of trees. The distinct shape of the waveform is a direct representation of tree distribution, density, and height variability within the footprint (Muss et al., 2013), all of which are critical components in calculating LE. By using these shape-based metrics, we assess the effect of tree distribution within each unit area on LE values.

$$RG = \sqrt{\frac{(x_i - C_x)^2 + (y_i - C_y)^2}{n}} \tag{5}$$

To evaluate the response of the LE to variations in relative height (RH) values across different ecological stages, we conduct a local sensitivity analysis (Hamby, 1994; Borgonovo and Plischke, 2016). This approach was chosen for its suitability in studies of environmental modeling, where it helps in understanding system behavior under slight changes in input parameters (Saltelli et al., 2000; Xu et al., 2004). Therefore, sensitivity was calculated as the change in Lorenz entropy relative to the change in RH values using the following formula (Eq. (6)):

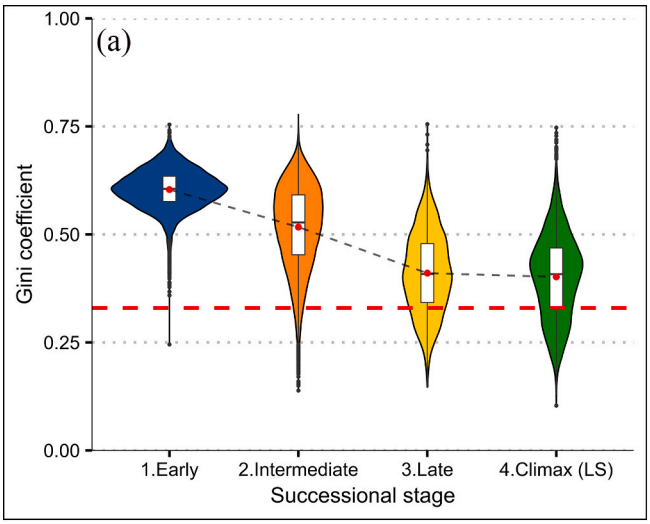


One-way ANOVA Test

| df | Mean Square | F | Pr(>F) |
|---|---|---|---|
| 3 | 107.98 | 11,383 | <2e-16 |

Tukey Post Hoc Test comparisons of means in 95% family-wise confidence level

| Successional stage | Diff. in means | Adjusted P-value | Effect size |
|---|---|---|---|
| Early - Intermediate | $-8.68\times 10^{-2}$ | <0.001 | -0.93 |
| Early - Late | $-1.93\times 10^{-1}$ | <0.001 | -2.58 |
| Intermediate - Late | $-1.07\times 10^{-1}$ | <0.001 | -1.11 |
| Late - Climax | $-8.70\times 10^{-3}$ | <0.001 | -0.09 |

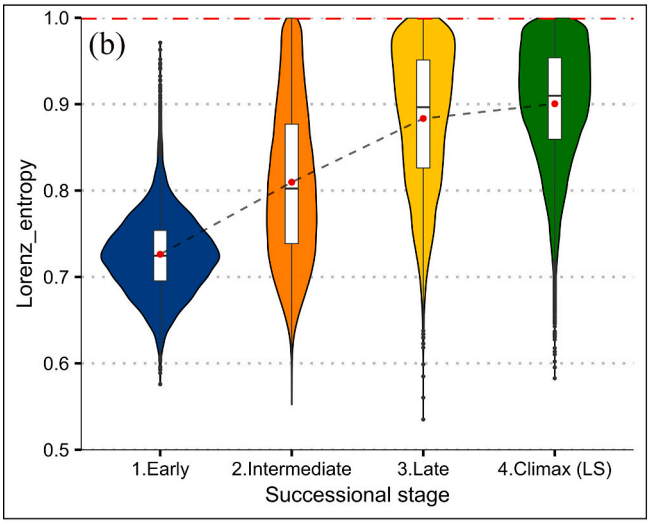


One-way ANOVA Test

| df | Mean Square | F | Pr(>F) |
|---|---|---|---|
| 3 | 76.97 | 11,425 | <2e-16 |

Tukey Post Hoc Test comparisons of means in 95% family-wise confidence level

| Successional stage | Diff. in means | Adjusted P-value | Effect size |
|---|---|---|---|
| Early - Intermediate | $8.35\times 10^{-2}$ | <0.001 | 0.95 |
| Early - Late | $1.73\times 10^{-1}$ | <0.001 | 2.80 |
| Intermediate - Late | $8.98\times 10^{-2}$ | <0.001 | 1.05 |
| Late - Climax | $1.70\times 10^{-2}$ | <0.001 | 0.25 |

**Fig. 5.** Successional stage vs. the Gini coefficient (a) of different study sites. The analysis of variance table and Tukey post hoc test between different successional stages group (early, intermediate, late, and climax) and the Gini Coefficient (GC) represents the significant differences between these stages. It is evident that as the forest grows from early to climax, the Gini coefficient's mean value (red dot) decreases to 0.33. Simultaneously, the successional stage vs. the Lorenz-entropy (b) increased to 1 and the analysis of variance table and Tukey post hoc test prove the significant differences between the corresponding successional stages. The red dashed line in each plot represents the maximum entropy of the Gini coefficient (a) and the maximum Lorenz-entropy (b), and the red dots are the mean values of the corresponding Gini coefficient and Lorenz- entropy. The black dashed line shows the trend of mean values in (a) and (b). (For interpretation of the references to colour in this figure legend, the reader is referred to the web version of this article.)

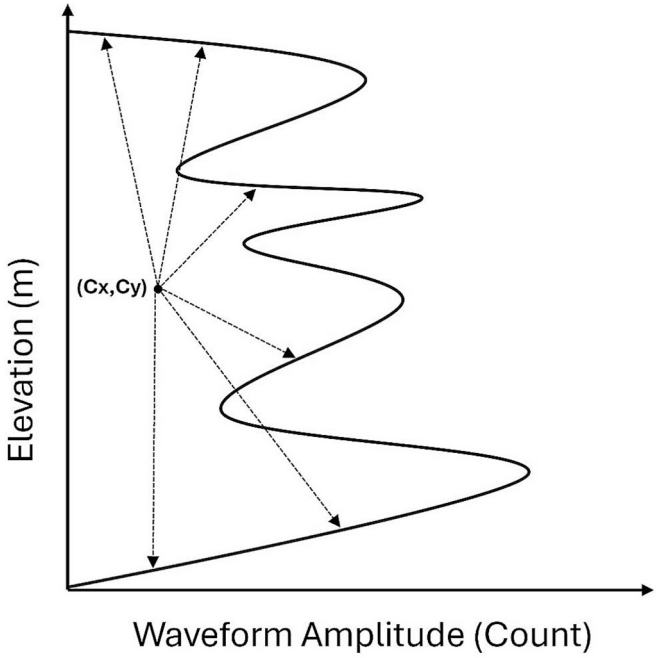


**Fig. 6.** The centroid ($C_x$, $C_y$), and the Radius of Gyration (RG), based on waveform amplitude (Gu et al., 2018).

**Table 1**
The description of shape-based metrics, WAF is waveform amplitude figure.

| Type | Acronym | Source | Description |
|---|---|---|---|
| Shape-based | Cx | WAF | The x coordinate of the waveform centroid |
| | Cy | | The y coordinate of the waveform centroid |
| | RG | | The radius of gyration, is the root mean square of the sum of the two-dimension distances that all points on the waveform are from its centroid |

$$\text{Sensitivity} = \frac{\Delta LE}{\Delta RH} \tag{6}$$

Where ΔLE is the difference in the LE between consecutive observations, and ΔRH is the corresponding difference in RH values. For each successional stage, we computed the sensitivity of LE against all the RH metrics (from RH_0 to RH_100). Only valid consecutive observations with non-zero changes in RH ($\Delta RH \neq 0$) were included to avoid division by zero errors. For each valid pair, the sensitivity was calculated, and the mean sensitivity across all pairs was determined as (Eq. (7)):

$$\text{Average sensitivity} = \frac{1}{n}\sum_{i=1}^{n}\frac{\Delta LE_i}{\Delta RH_i} \tag{7}$$

where n is the number of valid observations as indicated above.

### 2.8. Biomass and basal area

To validate the result from the LE, we used the inventory data from two- and three- dimensional (BA, and biomass) forest metrics were procured from the SRNP-EMSS 2005 annual forest inventory (Calvo-Rodriguez et al., 2021), and subsequently utilized Chave et al. (2014) to estimate forest biomass at the three distinct stages at the SRNP-EMSS (Calvo-Rodriguez et al., 2021). The biomass estimation for La Selva Biological Station (LS), as climax stage, was taken from Meyer et al. (2018), which used the Brown et al. (1989) and Gibbs et al. (2007) allometric models to derive the biomass (Supplementary Table 5). The BA data was taken from (Clark et al., 2021). To confirm the observed trend in the LE, we conducted a comparative analysis of biomass and basal area (BA) distributions across different stages, employing both violin and boxplot visualizations. Furthermore, to illustrate alterations in the GC of inventory data—specifically biomass and basal area—a Lorenz curve was constructed.

### 2.9. Heatmaps from the Lorenz-entropy and the Gini coefficient

Using the data from the LE and the GC, which were quantified from waveform LiDAR, we collected the data across various sample plots representing different stages of ecological succession. The analytical process involved creating heatmaps using Surfer, a scientific visualization software designed for geospatial data analysis (*Golden Software*, 2024). This software was used to transform the LE and GC data into a grid or raster format. The transformation process involved using advanced interpolation methods, particularly kriging, a geostatistical technique for accurately predicting continuous spatial variables from discrete data points. The kriging process required fine-tuning various parameters, such as range, sill, and nugget, to ensure that the interpolated surface was smooth and accurately reflected the underlying spatial patterns in the data (Chilès and Desassis, 2018).

## 3. Results

In our study, we explored the application of airborne waveform LiDAR technology (LVIS) to develop an entropy-based indicator to evaluate the vertical structural diversity and complexity of tropical forest ecosystems. The two- (Basal area), and three- (Biomass) dimensional forest metrics utilizing to validate the result.

### 3.1. Waveform LiDAR and Lorenz-entropy

Fig. 4 represents the effective LiDAR waveform (Fig. 4a) from the LVIS, the normalized cumulative return energy (Fig. 4b), and the Lorenz curve for each 20-m footprint data (Fig. 4c) that were generated for all successional stages. From the waveforms in this figure, we could easily distinguish the differences in the number of peaks, relative heights, and Lorenz curve shapes for each stage. Here, the GC was calculated based on the Lorenz curve and the differences between the GC values for each footprint are visible through the area between the Lorenz curve and line of equality (dashed line).

### 3.2. Statistical analysis

The one-way ANOVA analysis, *p*-value (<2e-16) indicates that there is a statistically significant difference among at least one pair of successional stages in both the GC and the LE indicators (GC: $F = 11{,}383$, $p < 2e\text{-}16$; LE: $F = 11{,}425$, $p < 2e\text{-}16$). A subsequent Tukey post-hoc test was performed to ascertain the specific groups between which these significant differences occur. The outcomes of this test, conducted with a significance level of $\alpha = 0.05$ and yielding a p-value of 0.0, indicate statistically significant differences in both the LE and the GC between all pairs of stages. These differences are illustrated in Fig. 5a and b and further elaborated in Supplementary Tables 1 and 2. The mean difference between the climax and late stages for the GC ($-8.70 \times 10^{-3}$) and the LE ($1.70 \times 10^{-2}$), indicating that these two stages have very similar values. Additionally, the effect size between the late and climax stages is small ($d = 0.25$), suggesting a relatively minor difference in the LE and the GC between these two stages, despite a statistically significant difference detected by ANOVA. A large effect size is observed between the early and late stages ($d = 2.80$), indicating substantial differences in the LE between the early and late stages. An effect size of −0.09 is indicating that the difference in the GC between the late and climax stages is very small. This suggests that the structural inequality (as measured by the GC) is quite similar between the two stages.

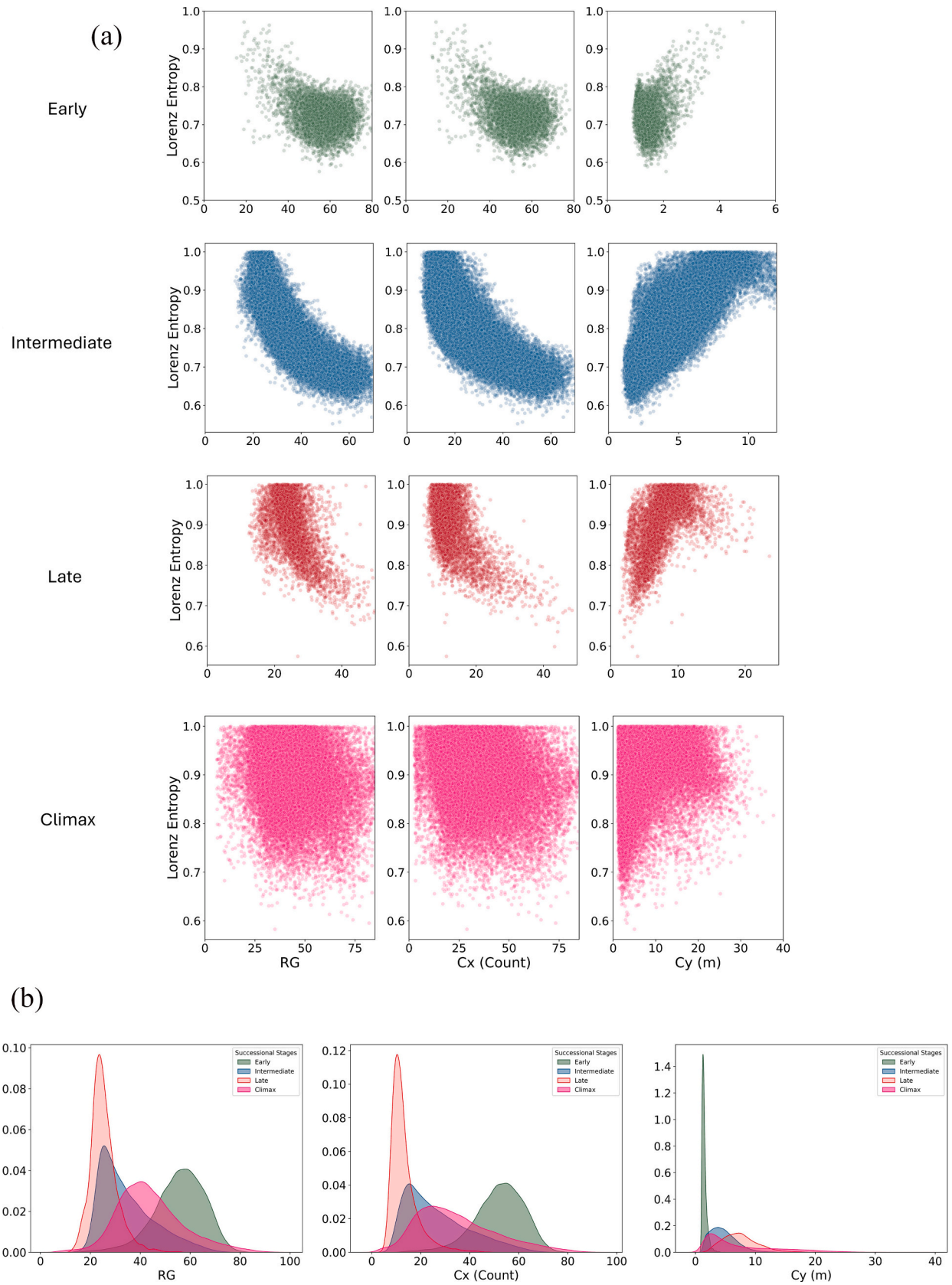


**Fig. 7.** The scatter plot of shape-base LiDAR metrics (RG, Cx, and Cy) and Lorenz-entropy (LE) (a) and the density plot of these metrics (b) along the different successional stages (early, intermediate, late, and climax). The Cx, is the x coordinate of the waveform centroid, the Cy is the y coordinate of the waveform centroid, and the RG is the Radius of Gyration.

**Table 2**
Mean sensitivity of Lorenz Entropy (LE) to RH metrics across successional stages.

| Successional stage | Mean sensitivity |
|---|---|
| Early | 1.78 |
| Intermediate | 2.06 |
| Late | 1.89 |
| Climax | 1.42 |

### 3.3. Characterizing Lorenz-entropy relative to the scale and waveform

Fig. 7a represents the relationship between shape-based metrics, Cx, Cy, and RG with LE across different successional stages, highlighting how variations in the waveform shape influence entropy values. The waveform amplitude distribution within each footprint determines the centroid positions (Cx and Cy) and the RG, indicating the spread and density of the canopy structure.

The Cx metric, representing the x-coordinate of the waveform centroid, decreases due to increased foliage density and reduced amplitude variability as the canopy becomes denser and more homogeneous. In contrast, the Cy metric, which represents the y-coordinate of the waveform centroid, increases as the forest matures, indicating a rise in average canopy height and vertical complexity (Fig. 7a and b). This change in amplitude distribution also results in a decrease in RG, reflecting a more compact canopy structure with less dispersion of foliage (Liu et al., 2023, Fig. 7b).

The sensitivity analysis revealed how the LE responds to changes in RH across the four ecological stages: early, intermediate, late, and climax. The mean sensitivity values, which represent the average response of LE to changes in RH metrics at each stage, are summarized in the Table 2.

Intermediate stage exhibited the highest mean sensitivity (2.06), indicating that LE in this stage is the most responsive to changes in RH values. However, climax stage showed the lowest mean sensitivity (1.42), implying that LE is less affected by RH changes at this stage. Moreover, late and early stages displayed moderate sensitivity, with mean values of 1.89 and 1.78, respectively.

### 3.4. Structural diversity and inequality

The analysis of the Lorenz curve derived from the airborne waveform LiDAR revealed a discernible pattern: as forests advance towards the climax stage, the mean value of the GC, approaches 0.33 (the MAXENT of GC for the one-dimensional metric (canopy height)). This finding, depicted in Fig. 5a with the red dashed line, symbolizes a trend towards uniformity in the canopy height distribution. The convergence of the mean GC value towards 0.33 indicates a decrease in canopy height diversity, suggesting a transition towards a more homogenized forest structure. This homogenization is characterized by less variance in canopy heights (high uniformity), signalling a move towards ecological evenness within the climax forest stage (Ehbrecht et al., 2021).

### 3.5. The Lorenz-entropy vs the Gini coefficient

Based on the evaluation of Fig. 5, it can be discerned that in diagram 6a, the GC transitions from the early to the climax stage, achieving a value of approximately 0.33. Conversely, in diagram 5b, within the same temporal sequence, the LE index monotonically increased (mean values) and reach plateau at climax stage and 1, representing the peak of this index. This increment signifies that the ecosystem has attained its climax phase, characterized by peak complexity and structural heterogeneity. Ideally, this culmination promotes enhanced productivity until the ecosystem arrives at a dynamic equilibrium, displaying a stabilized state, particularly in tropical forest ecosystems (Chitale et al., 2012; Schnabel et al., 2019, Supplementary Fig. 1).

### 3.6. Validation of the Lorenz-entropy

Fig. 8 is representing the results of analysis the inventory data which indicates the trends in biomass and Basal Area (BA) across different successional stages within the SRNP-EMSS and La Selva Biological Station. This analysis clarifies the relationship between the LE, quantifying by using airborne waveform LiDAR technology, and forest's two- and three-dimensional structural components (BA and biomass). BA as two-dimensional and biomass as three-dimensional variables were measured from inventory data from early to climax successional stages. The findings suggest a positive correlation between the increase in LE—from early successional stages to climax—and the increase in biomass and BA. Higher biomass and BA values indicate stand density and the distribution of tree sizes within a forest ecosystem (Enquist and Niklas, 2001; Arcanjo and Torezan, 2022). These values suggest denser forests, characterized by more prominent and numerous trees, and play a key role in determining forest productivity (Luo et al., 2023). In addition, in Fig. 8 the Lorenz curve, which represents the variation in the Gini Coefficient (GC) across different stages is added. By quantifying the GC and the LE from inventory data, as outlined in our conceptual model (shown in Fig. 2), we can determine if the studied plots result from the nuclear tree's advancement or the natural proliferation from zero forests. Table 3 delineates the GC and LE values as deduced from these analyses. From these calculations, we can infer that these plots predominantly occupy the left segment of the graph, indicating their derivation from zero forests. However, it is important to acknowledge that these are representative sample plots from our study areas intended to illustrate the fluctuations in the GC and LE according to actual measurements.

Moreover, Fig. 9 shows the variations in LE and the GC across different forest successional stages in plot level. The heat maps generated for this analysis were based on data collected from various plots within both study areas. These heat maps revealed a trend: as the successional stage progresses from early to climax, the intensity of the GC decreases, whereas the intensity of the LE increases, moving towards its maximum value of 1. This pattern underscores the dynamic nature of forest ecosystems, highlighting how, as forests mature, the structural complexity and entropy of the system intensify.

## 4. Discussion

### 4.1. Advantages of Lorenz-entropy

Vertical structural complexity and structural diversity play a key role in understanding ecosystem health and resilience, as they are closely linked to biodiversity, productivity, and the capacity of ecosystems to withstand disturbances (Edeline et al., 2023; Madin et al., 2023). Remote sensing techniques are valuable for gathering this information on ecosystem function and biodiversity (Beland et al., 2019; Bush et al., 2017). In this research, we used airborne waveform LiDAR data to measure and demonstrate the structural diversity and complexity in tropical forests using the Lorenz-entropy (LE) index. Our results indicated that the proposed LE index is capable to indicate variations in vertical structure and can detect changes across ecological successions in tropical forests' LiDAR footprints (Fig. 5a and b) and the plot level (Figs. 8 and 9). Previous studies by Aoki (1995), Fath et al. (2004), and Cushman (2018) predicted the behavior of entropy at different growth stages of ecosystem using only mathematical approaches. However, the LE index proves its ability to demonstrate entropy trends and uncertainty across a chronosequence of a tropical dry forest and in a climax rainforest (Fig. 5b). The LE reflects its capacity to quantify the entropy across different dimensions of forest metrics (canopy height (one-dimension), basal area (two-dimension), and biomass (three-dimension), Fig. 8a and b). Another advantage of the LE index is its capability to trace back the ecological process of succession in tropical forests, supporting the findings of Janzen (1988) (Fig. 2). Prior studies (Macarthur and Macarthur, 1961; Cushman, 2021) only calculated

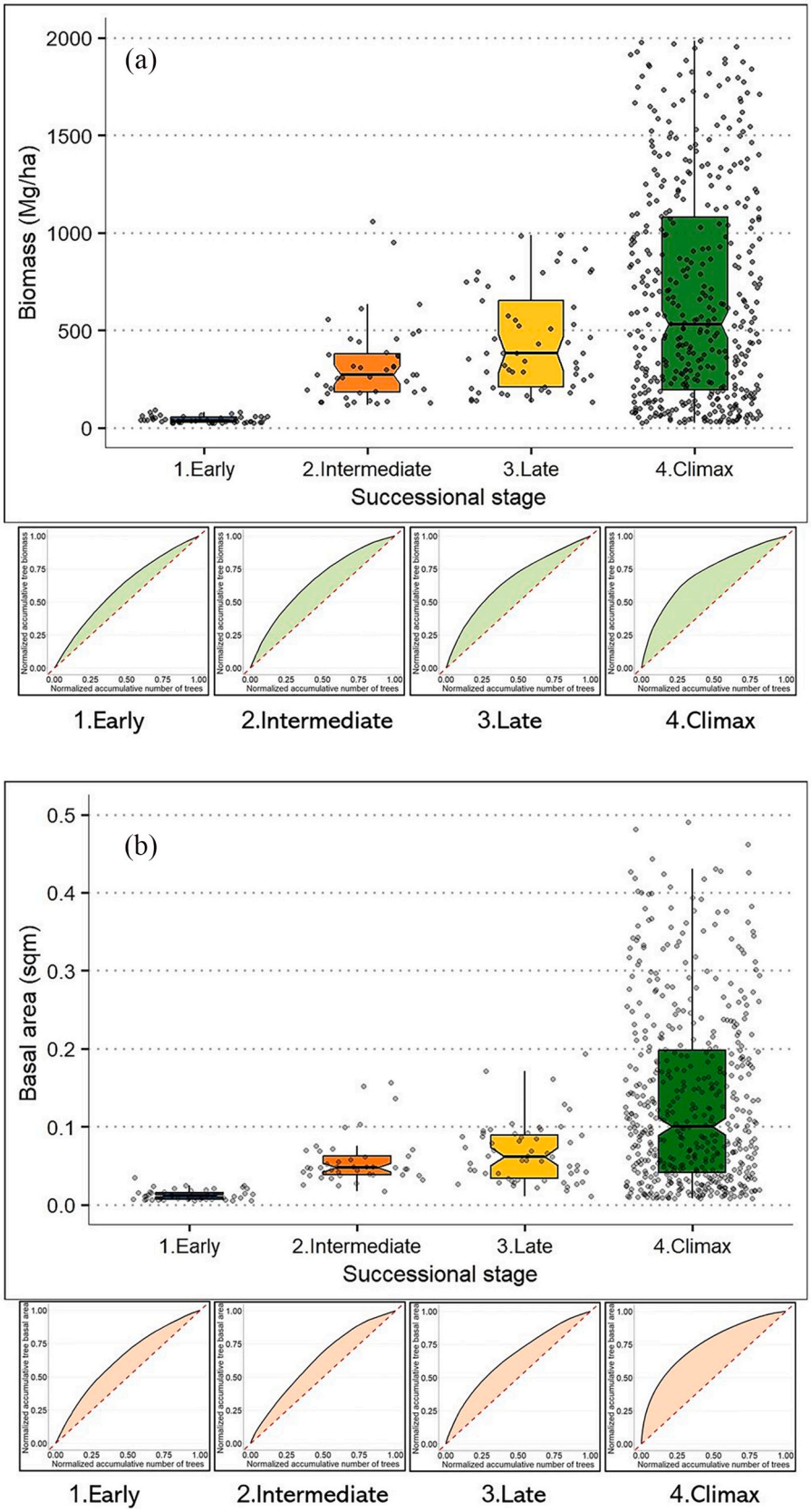


**Fig. 8.** The evolution of inventory biomass (a) and basal area (b) data from the Santa Rosa National Park (early, intermediate, and late) and La Selva Biological Station as the climax stage. This trend is aligned with the changes in the entropy as indicated by the developed Lorenz-entropy index, which reveals an increase in biomass and basal area from the early to climax stages. The corresponding Lorenz curve from biomass and basal area from the inventory data is created, representing the trend in changing the area between the Lorenz curve and the line of equality (red dashed line) representing the Gini coefficient (GC), in different successional stages. (For interpretation of the references to colour in this figure legend, the reader is referred to the web version of this article.)

**Table 3**
The Gini Coefficient (GC), and the Lorenz-entropy (LE) values, calculated from basal area and biomass inventory data for early, intermediate, and late successional stages of SRNP-EMSS, and climax stage of La Selva Biological Station.

| Successional stage | GC from basal area ($MAXENT_{GC=0.50}$) | GC from biomass ($MAXENT_{GC=0.60}$) | LE from basal area | LE from biomass |
|---|---|---|---|---|
| Early | 0.26 | 0.22 | 0.76 | 0.56 |
| Intermediate | 0.27 | 0.32 | 0.77 | 0.66 |
| Late | 0.31 | 0.33 | 0.81 | 0.67 |
| Climax | 0.50 | 0.44 | 1 | 0.78 |

entropy using the FHD and Shannon entropy formula without empirically demonstrating its measurement. However, in this study, we used the LE index to measure uncertainty in structural complexity, which represents the significant differences across various dimensions of forest metrics and successional stages (see Figs. 5 and 8).

Other entropy-based indices, specifically the Shannon Entropy Index (SEI, Shannon, 1948), are often used to measure diversity; however, they have limitations in accounting for the distribution and arrangement of species or elements within an ecosystem (MacDonald et al., 2017; Roswell et al., 2021). The SEI does not consider the ecological characteristics of forest ecosystems and may not reflect the importance of specific species or elements within a given ecosystem (Jost, 2006). As a result, in this research, we tried to address these gaps by introducing a LiDAR waveform-based entropy index that incorporates practical implications for forest ecology such as enhancing monitoring of tropical forest ecosystems. Moreover, the recent entropy-based method developed by Liu et al. (2022), for quantifying vertical and horizontal forest canopy structural complexity; However, it also has certain limitations. The key limitation is the potential variability in data quality and resolution from different Lidar platforms, which can introduce inconsistencies in the analysis. Additionally, the method relies heavily on the accurate alignment and integration of data from multiple sources. Moreover, by using TLS, the spatial coverage is limited due to the fixed position of the scanner and the relatively small area that can be surveyed from each scanning position. In our research, we overcome these challenges of data variability and spatial coverage by employing airborne LiDAR technology. This technology provides consistent and extensive spatial coverage, which allows us to generate more uniform and consistent datasets.

### 4.2. The Lorenz-entropy vs the Gini coefficient

The LE formula is a function of the GC, defined through their mathematical relationship as presented in Eq. (1). While GC measures inequality, the transformation from GC to LE is grounded in the i) ecological application of the second law of thermodynamics (entropy), indicated by Svirezhev (2000) and Nielsen et al. (2020), ii) structural complexity (Liu et al., 2022; Weiner and Solbrig, 1984), and iii) ecological successional theory (Janzen, 1988) rather than being merely a statistical reformulation without physical meaning. This makes the LE a robust metric for describing structural diversity and complexity in forest ecosystems. For example, in our analysis of successional stages, in a tropical dry and a tropical rain forest using actual data, the LE effectively distinguished the increasing entropy and complexity as a function of ecological succession (Fig. 5b). In contrast, while the GC can classify the different successional stages (Fig. 5a), it could not define the differences of successional trajectories, influenced by forest origin processes (e.g., wind dispersed vs vertebrate dispersed), as discussed by Janzen, 1988. Studies by Castillo-Núñez et al. (2011) and Castillo et al. (2012) which utilized LiDAR data, further demonstrated the significance of these successional processes for understanding forest recovery in tropical ecosystems.

The LE's utility extends to detailed assessments of forest dynamics and entropy, whereas GC provides a snapshot of evenness and inequality (Valbuena, 2015; Valbuena et al., 2016). LE offers a broader perspective on forest succession by capturing entropy-driven transitions across successional stages, as demonstrated in Fig. 5b with data from a tropical dry and a tropical rain forest. This makes the LE particularly valuable for studies investigating the interplay between structural complexity, and forest recovery.

### 4.3. Contribution to evenness and structural complexity

The outcomes of our study provide substantial contributions to the comprehension of evenness and structural complexity within tropical forest ecosystems. This is achieved through utilizing the GC, an indicator for assessing ecosystem inequality. The significance of GC derives from its role as a summary statistic for the Lorenz curve, which enhances our grasp of plant size distributions and structural complexity (Weiner and Solbrig, 1984; Damgaard and Weiner, 2000), as explained through LiDAR data (Fig. 5a).

Empirical support for the applicability of the GC to assess structural diversity within forests has been highlighted in previous studies (Valbuena et al., 2016; Valbuena et al., 2012). The advantages of the GC include its logical ranking of distributions and sensitivity to varying sample sizes (Wright Muelas et al., 2019; Blesch et al., 2022), making it a valuable tool.

Recent developments in ecological equations of state have provided insights into the relationship between species diversity and other ecosystem characteristics (Harte et al., 2022). However, these approaches often need to be revised in terms of scale. In our research, the LE index aims to address this issue by acquiring footprints of airborne LiDAR and spatially explicit LiDAR technology over swaths of forest cover, rather than using just sample data.

As an ecosystem reaches a climax stage, a balance exists where a greater variety of species coexist and resources are more evenly distributed (Brun et al., 2019). This reduces inequality and increases evenness (Jost, 2010; Hordijk et al., 2023). Our study shows this through the decreasing trend of the GC towards 0.33. The relationship between evenness and complexity is critical in understanding the stability and resilience of tropical forests (Hill, 1973; Kvålseth, 1991). A higher evenness suggests a more equal resource distribution and greater ecosystem resilience in the face of disturbances. This suggests greater biodiversity can improve an ecosystem's overall functioning and services (Hong et al., 2022). Moreover, high evenness suggests a more equitable distribution of species abundance, which may enhance resource utilization efficiency and promote stability within the ecosystem (Stirling and Wilsey, 2001; Hordijk et al., 2023). Tuomisto and Tuomisto (2012) and Yan et al. (2023a, 2023b) suggest that understanding the intricate relationships between species richness, evenness, and proportional diversity requires a thorough investigation across different ecological contexts for explaining ecosystem dynamics. To support this, our proposed LE index provides a solution for elucidating the role of evenness in complementing richness and productivity in tropical forest ecosystems through an empirical study using essential forest variables, such as canopy height, basal area, and aboveground biomass.

### 4.4. Lorenz-entropy and successional stages

One important application of this study is using the LE to assess the forest's conditions along chronosequence, given changes in the diversity, structure and composition over time (Guariguata and Ostertag, 2001; Lohbeck et al., 2012).This scenario culminates in a climax stage, where the species composition is relatively stable, and the community is in equilibrium with the prevailing environmental conditions. The dominant species in a climax forest are typically long-lived and well-adapted to the local climate, soil, and other environmental factors (Hartshorn, 1980). This is where these characteristics (diversity and

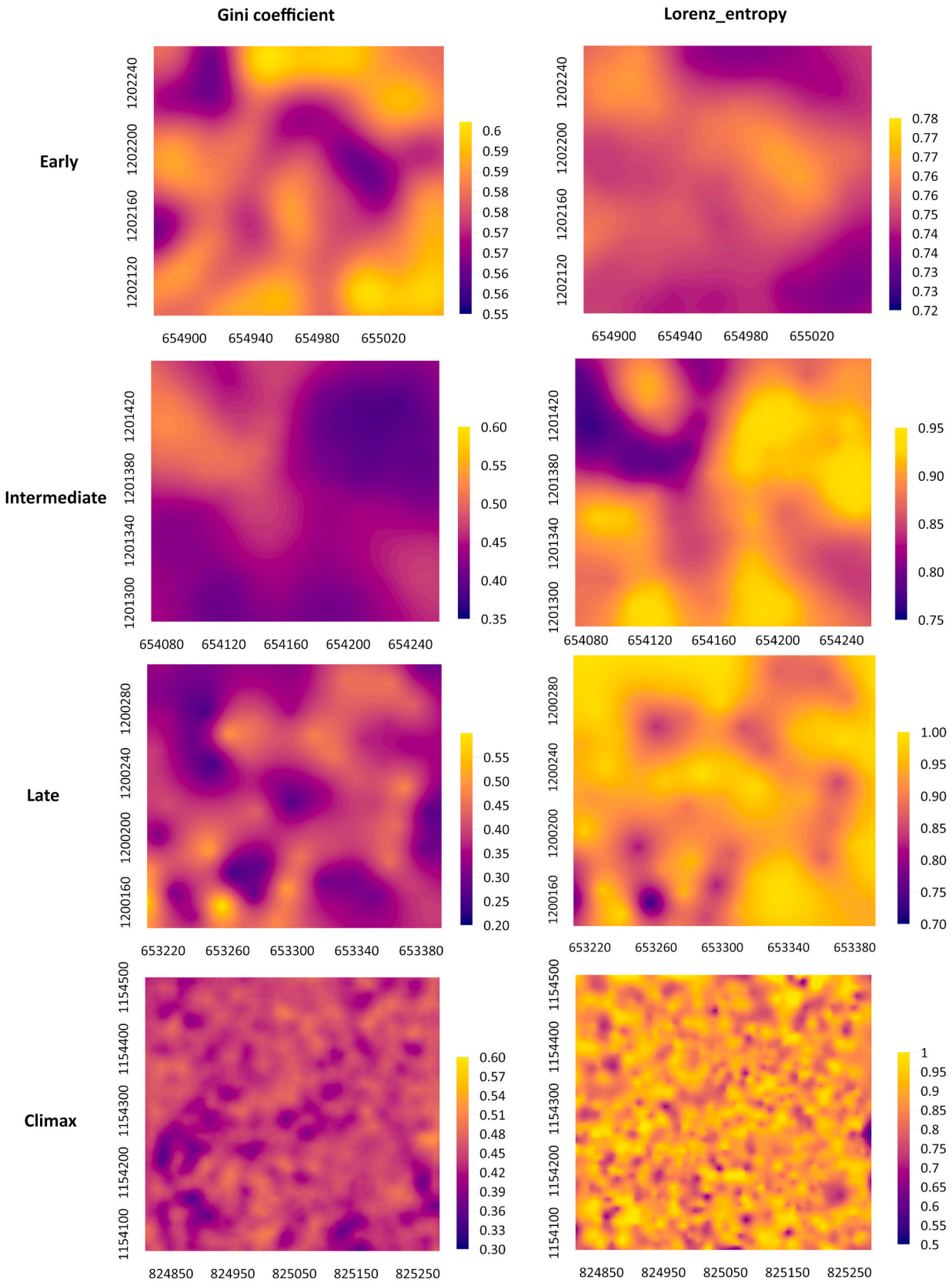


**Fig. 9.** Heatmap of the Lorenz-entropy (LE) and the Gini coefficient (GC) at the SRNP-EMSS for early, intermediate, and late stages, and La Selva for the climax stage. This figure represents the intensity of the GC and the LE across different stages of ecological succession.

composition) are at their highest. This transformation results from interactions between ecological development, biodiversity expansion, and inequality dynamics (Tilman et al., 2014; Guralnick et al., 2015).

The results of the statistical analysis indicate that, although there are statistically significant differences between the late and climax stages of forest succession, the magnitude of these differences is relatively small, as reflected by the small effect size (Cohen's d = 0.25). This finding supports our interpretation and hypothesis that Lorenz-entropy (LE) increases substantially from the early to late stages and then stabilizes as the forest reaches the climax stage and the GC value tends to converge towards 0.33 for one-dimensional forest metric (canopy height), Adnan et al. (2021). While the differences between the late and climax stages are statistically significant, they are less meaningful in practical terms due to the observed small effect size. In fact, these results suggest that the late and climax stages are highly similar in terms of vertical structural complexity and entropy (Fig. 5). This observation is consistent with the perspective that the climax stage represents an extension or stable phase of the late successional stage, rather than a distinct stage with unique structural characteristics (Guariguata and Ostertag, 2000; Poorter et al., 2016; Rozendaal et al., 2019).

While this study focuses on 20-m footprints obtained from LVIS data, the methodology can be extended to other spatial scales, including spaceborne LiDAR datasets such as GEDI, as long as full waveform data are available. This flexibility underscores the robustness of the LE index in capturing entropy across varying resolutions and scales. As the findings from LiDAR shape-based metrics revealed the impact of these metrics (Cx, Cy, and RG) on LE, which is evident as the forest moves from one successional stage to another (Fig. 7). In the early stages, a more heterogeneous amplitude distribution leads to lower LE values due to greater variability in canopy structure. As the forest develops and canopy gaps close, the amplitude distribution becomes more homogeneous, causing an increase in LE. This transition is captured by the decreasing Cx values, which reflect a reduction in amplitude variation within each footprint. The increasing trend in Cy indicates a higher vertical structure, which stabilizes in the climax stage, reflecting the uniformity and complexity of the mature forest canopy. Simultaneously, the reduction in RG values signals a more compact canopy structure, indicating a shift towards uniformity and stability in the forest's vertical complexity. At the climax stage, these trends stabilize, indicating that the canopy structure has reached equilibrium, and further changes in Cx, Cy, or RG are minimal. The lack of variation in these metrics suggests that the Lorenz-entropy (LE) has reached a plateau, capturing the uniformity and structural stability of the mature forest. This behavior aligns with the expectations for climax-stage forests, where structural complexity and vertical stratification are at their maximum, and further entropy increases are limited (Petrokas, 2020; Pos et al., 2023).

The sensitivity analysis indicated the responses of the LE in changing in the RH metrics from the LVIS in different successional stages (Table 2). The intermediate stage exhibited the highest sensitivity, suggesting that canopy structure during this phase is more dynamic, with significant fluctuations in vertical distribution. This increased sensitivity in the intermediate stage can be attributed to greater species turnover, mortality, and liana density (Kalácska et al., 2005; Calvo-Rodriguez et al., 2021; Duan et al., 2023).

In contrast, the climax stage showed the lowest sensitivity, reflecting the stability and equilibrium of mature forests. At climax stage, canopy height changes have a minimal impact on LE, suggesting that the forest's structural complexity has reached a relatively stable state which aligns with our results from Fig. 5(b).

The early and late stages displayed moderate sensitivity, suggesting that these stages are characterized by ongoing structural development, but with less pronounced changes compared to the intermediate phase. The early stage reflects the initial establishment of canopy layers, while the late stage shows a gradual approach to maturity.

### 4.5. Limitation of the current study

Despite its outstanding utility, the Lorenz curve may not fully summarize the complexity of biomass distribution patterns, particularly in instances where ecological processes interact nonlinearly or exhibit spatial heterogeneity. Our study did not incorporate trees' spatial coordinates (x and y positions) within the different successional stages. This limitation could impact the spatial distribution patterns in forest structure and dynamics. The Lorenz curve graphical representation provides two distinct scenarios of forest structure when dealing with this limitation regarding biomass: one characterized by a biomass distribution predominantly influenced by a larger number of individuals, and another one marked by a domination of biomass by a smaller cohort of individuals (Supplementary Fig. 2). This duality of the Lorenz curve underscores the intricate growth dynamics inherent in tropical forest ecosystems, where diverse biomass accumulation and distribution patterns manifest as the original pass of succession. Therefore, while the index and accompanying visual aids provide valuable insights into broad-scale trends, they may fail to capture differences in biomass allocation and ecological dynamics.

Another important aspect of developing the LE index is normalizing the cumulative height profile to the [0,1] range. While this normalization preserves the variability information of the height profile, it can result in Lorenz curves for different forest canopy heights appearing identical, regardless of their actual heights. Consequently, this can obscure differences between taller and shorter canopies, indicative of greater structural complexity. To address this issue, it is important to complement the LE index with a measurement of absolute canopy height or another relevant metric. This approach will help distinguish between different canopy heights and provide a more accurate assessment of forest structural complexity.

Future index improvements could involve integrating additional metrics or employing advanced modeling techniques to better account for such complexities and enhance the index's discriminatory power across diverse ecological contexts. Moreover, our future research aims to answer whether the LE index effectively captures the complex entropy and structural diversity variations across different tropical forests. Given the wide range of ecological features in tropical forests-including species composition, vegetation structure, and environmental conditions-assessing the index's ability to discern these differences is crucial for establishing its validity and robustness. This investigation will contribute significantly to the global applicability of the LE index in tropical forest research.

## 5. Conclusion

In this research we developed an entropy-based index (LE index) to measure the structural complexity and structural diversity in tropical forests. The integration of various disciplines, and advanced analytical remote sensing techniques presented in this study were proposed to address the limitations of existing indices in capturing the intricate structural variations and ecological dynamics within these ecosystems.

Using empirical data, this study advances our understanding of the linkage between vertical structural complexity, structural diversity, and productivity in tropical forest ecosystems. The results reveal that as tropical forests progress through different successional stages towards the climax stage, structural complexity increases while canopy height inequality decreases. The LE index, peaking at 1 in the climax stage, indicates maximum structural heterogeneity and complexity. The Gini Coefficient (GC) trends towards 0.33, reflecting a more uniform distribution of canopy heights and suggesting that mature forests exhibit greater ecological evenness. LiDAR-derived shape-based metrics (Cx, Cy, RG) effectively captured the structural changes within forest canopies, with Cx decreasing and Cy increasing as forests mature. These metrics, in conjunction with LE, provide a robust framework for assessing vertical complexity and canopy distribution across ecological

succession.

The sensitivity analysis conducted in this study revealed that the response of LE to changes in RH metrics varies across successional stages. Intermediate stages exhibited the highest sensitivity, reflecting greater fluctuations in canopy height and more dynamic forest structures. In contrast, the climax stage showed the lowest sensitivity, indicating that canopy structure stabilizes as forests reach maturity, with minimal impact on LE from further height variations. Early and late stages displayed moderate sensitivity, representing ongoing but less pronounced structural development.

The validation of the LE index using biomass and basal area (BA) measurements further supports these trends, showing a positive correlation between increasing LE values and higher biomass and BA in the forest. Spatial heatmaps illustrate that the intensity of the LE index increases with forest succession, reinforcing the observed patterns of rising structural complexity and evenness. We suggest that the proposed LE index has the potential to contribute to a deeper understanding of ecological communities and forest dynamics at tropical forests' landscapes.

## Funding statement

The study was supported by a discovery grant from the Natural Sciences and Engineering Research Council of Canada (NSERC).

## Ethical compliance

This research is not included studies on human subjects, human data or tissue, or animals.

## Author contribution

Nooshin Mashhadi contributed to the design and development of methodology, analysis, and validation of the results, and writing of the manuscript. Dr. Arturo Sanchez-Azofeifa with the main idea, its conceptualization, review writing, and editing, and supervised the project. Dr. Ruben Valbuena to the validation of the mathematical component, review and editing of the manuscript. The three authors jointly contributed to the development of the Lorenz-entropy index.

## CRediT authorship contribution statement

**Nooshin Mashhadi:** Writing – review & editing, Writing – original draft, Visualization, Validation, Software, Resources, Project administration, Methodology, Formal analysis, Data curation, Conceptualization. **Arturo Sanchez-Azofeifa:** Writing – review & editing, Visualization, Validation, Supervision, Project administration, Methodology, Funding acquisition, Formal analysis, Data curation, Conceptualization. **Ruben Valbuena:** Writing – review & editing, Validation, Methodology, Formal analysis.

## Declaration of competing interest

The authors declare the following financial interests/personal relationships which may be considered as potential competing interests.

Arturo Sanchez-Azofeifa reports was provided by Natural Sciences and Engineering Research Council of Canada (NSERC). If there are other authors, they declare that they have no known competing financial interests or personal relationships that could have appeared to influence the work reported in this paper.

## Acknowledgments

The authors would like to express their appreciation to the Center of Earth Observation Science at the University of Alberta and the Department of Forest Resource Management at the Swedish University of Agricultural Sciences for their unwavering support and resources, which were instrumental in the completion of this research. This work was supported by a Discovery Grant from the Natural Sciences and Engineering Research Council of Canada (NSERC).

## Appendix A. Supplementary data

Supplementary data to this article can be found online at https://doi.org/10.1016/j.rse.2024.114545.

## Data availability

The dataset supporting this study will be made available upon request. A brief code snippet demonstrating the calculation of Lorenz entropy from waveform LiDAR data is accessible at https://doi.org/10.5281/zenodo.14219678.

## References

Adnan, S., Maltamo, M., Mehtätalo, L., Ammaturo, R.N.L., Packalen, P., Valbuena, R., 2021. Determining maximum entropy in 3D remote sensing height distributions and using it to improve aboveground biomass modelling via stratification. Remote Sens. Environ. 260. https://doi.org/10.1016/j.rse.2021.112464.

Anderson, J., Martin, M.E., Smith, M.L., Dubayah, R.O., Hofton, M.A., Hyde, P., Peterson, B.E., Blair, J.B., Knox, R.G., 2006. The use of waveform lidar to measure northern temperate mixed conifer and deciduous forest structure in New Hampshire. Remote Sens. Environ. 105, 248–261. https://doi.org/10.1016/j.rse.2006.07.001.

Aoki, I., 1995. Entropy production in living systems: from organisms to ecosystems. Thermochim. Acta 250. https://doi.org/10.1016/0040-6031(94)02143-C.

Arcanjo, F., Torezan, J.M., 2022. Aboveground biomass accumulation and tree size distribution in seasonal Atlantic Forest restoration sites. Restor. Ecol. 31. https://doi.org/10.1111/rec.13669.

Arroyo Mora, J.P., Sánchez-Azofeifa, G.A., Rivard, B., Calvo, J., 2005. Quantifying successional stages of tropical dry forests using Landsat ETM. Biotropica 37, 497–507.

Atkins, J.W., Bhatt, P., Carrasco, L., Francis, E., Garabedian, J.E., Hakkenberg, C.R., Hardiman, B.S., Jung, J., Koirala, A., LaRue, E.A., Others, 2023. Integrating forest structural diversity measurement into ecological research. Ecosphere 14, e4633.

Beard, J.S., 1944. Climax Vegetation in Tropical America.

Beland, M., Parker, G., Sparrow, B., Harding, D., Chasmer, L., Phinn, S., Antonarakis, A., Strahler, A., 2019. On promoting the use of lidar systems in forest ecosystem research. For. Ecol. Manag. 450, 117484.

Bertram, J., 2014. Entropy-Related Principles for Non-equilibrium Systems: Theoretical Foundations and Applications to Ecology and Fluid Dynamics.

Blair, B., Rabine, D.L., Hofton, M.A., 1999. The laser vegetation imaging sensor: a medium-altitude, digitisation-only, airborne laser altimeter for mapping vegetation and topography. ISPRS J. Photogramm. & Remote Sens. 54 (2–3), 115–122.

Blesch, K., Hauser, O.P., Jachimowicz, J.M., 2022. Measuring inequality beyond the Gini coefficient may clarify conflicting findings. Nat. Hum. Behav. 6, 1525–1536. https://doi.org/10.1038/s41562-022-01430-7.

Borgonovo, E., Plischke, E., 2016. Sensitivity analysis: a review of recent advances. Eur. J. Oper. Res. 248, 869–887.

Brown, S., Gillespie, A., Lugo, A.E., 1989. Biomass Estimation Methods for Tropical Forests with Applications to Forest Inventory Data.

Brun, P., Zimmermann, N.E., Graham, C.H., Lavergne, S., Pellissier, L., Münkemüller, T., Thuiller, W., 2019. The productivity-biodiversity relationship varies across diversity dimensions. Nat. Commun. 10, 5691. https://doi.org/10.1038/s41467-019-13678-1.

Bush, A., Sollmann, R., Wilting, A., Bohmann, K., Cole, B., Balzter, H., Martius, C., Zlinszky, A., Calvignac-Spencer, S., Cobbold, C.A., Dawson, T.P., Emerson, B.C., Ferrier, S., Gilbert, M.T.P., Herold, M., Jones, L., Leendertz, F.H., Matthews, L., Millington, J.D.A., Olson, J.R., Ovaskainen, O., Raffaelli, D., Reeve, R., Rödel, M.O., Rodgers, T.W., Snape, S., Visseren-Hamakers, I., Vogler, A.P., White, P.C.L., Wooster, M.J., Yu, D.W., 2017. Connecting earth observation to high-throughput biodiversity data. Nat. Ecol. Evol. https://doi.org/10.1038/s41559-017-0176.

Cadotte, M.W., 2017. Functional traits explain ecosystem function through opposing mechanisms. Ecol. Lett. https://doi.org/10.1111/ele.12796.

Calvo-Rodriguez, S., Sánchez-Azofeifa, G.A., Durán, S.M., Do Espírito-Santo, M.M., Nunes, Y.R.F., 2021. Dynamics of carbon accumulation in tropical dry forests under climate change extremes. Forests 12, 1–15. https://doi.org/10.3390/f12010106.

Castillo, M., Rivard, B., Sánchez-Azofeifa, A., Calvo-Alvarado, J., Dubayah, R., 2012. LIDAR remote sensing for secondary tropical dry Forest identification. Remote Sens. Environ. 121, 132–143.

Castillo-Núñez, M., Sánchez-Azofeifa, G.A., Croitoru, A., Rivard, B., Calvo-Alvarado, J., Dubayah, R.O., 2011. Delineation of secondary succession mechanisms for tropical dry forests using LiDAR. Remote Sens. Environ. 115, 2217–2231.

Chave, J., Réjou-Méchain, M., Búrquez, A., Chidumayo, E., Colgan, M.S., Delitti, W.B.C., Duque, A., Eid, T., Fearnside, P.M., Goodman, R.C., Henry, M., Martínez-Yrízar, A., Mugasha, W.A., Muller-Landau, H.C., Mencuccini, M., Nelson, B.W., Ngomanda, A., Nogueira, E.M., Ortiz-Malavassi, E., Pélissier, R., Ploton, P., Ryan, C.M.,

Saldarriaga, J.G., Vieilledent, G., 2014. Improved allometric models to estimate the aboveground biomass of tropical trees. Glob. Chang. Biol. 20, 3177–3190. https://doi.org/10.1111/gcb.12629.
Chilès, J.P., Desassis, N., 2018. Fifty years of kriging. In: Handbook of Mathematical Geosciences: Fifty Years of IAMG. Springer International Publishing, pp. 589–612. https://doi.org/10.1007/978-3-319-78999-6_29.
Chitale, V.S., Tripathi, P., Behera, M.D., Behera, S.K., Tuli, R., 2012. On the relationships among diversity, productivity and climate from an Indian tropical ecosystem: a preliminary investigation. Biodivers. Conserv. 21, 1177–1197. https://doi.org/10.1007/s10531-012-0247-9.
Clark, David, Clark, Deborah, Kellner, J., 2021. Canopy height distributions and estimated above-ground biomass across a tropical rain forest landscape in Costa Rica, 1992-2018. https://doi.org/10.1002/ecm.1496.
Cohen, J., 1988. Statistical Power Analysis for the Behavioral Sciences Second Edition.
Coverdale, T.C., Davies, A.B., 2023. Unravelling the relationship between plant diversity and vegetation structural complexity: a review and theoretical framework. J. Ecol. https://doi.org/10.1111/1365-2745.14068.
Cushman, S.A., 2015. Thermodynamics in landscape ecology: the importance of integrating measurement and modeling of landscape entropy. Landsc. Ecol. https://doi.org/10.1007/s10980-014-0108-x.
Cushman, S.A., 2018. Calculation of configurational entropy in complex landscapes. Entropy 20. https://doi.org/10.3390/e20040298.
Cushman, S.A., 2021. Entropy in landscape ecology: a quantitative textual multivariate review. Entropy 23. https://doi.org/10.3390/e23111425.
Cushman, S.A., 2023. Entropy, ecology and evolution: toward a unified philosophy of biology. Entropy 25. https://doi.org/10.3390/e25030405.
Damgaard, C., Weiner, J., 2000. Ecological Society of America Describing Inequality in plant size or fecundity, source. Ecology. https://doi.org/10.1890/0012-9658(2000)081[1139:DIIPSO]2.0.CO;2.
De Boeck, H.J., Bloor, J.M.G., Aerts, R., Bahn, M., Beier, C., Emmett, B.A., Estiarte, M., Grünzweig, J.M., Halbritter, A.H., Holub, P., Jentsch, A., Klem, K., Kreyling, J., Kröel-Dulay, G., Larsen, K.S., Milcu, A., Roy, J., Sigurdsson, B.D., Smith, M.D., Sternberg, M., Vandvik, V., Wohlgemuth, T., Nijs, I., Knapp, A.K., 2020. Understanding ecosystems of the future will require more than realistic climate change experiments – A response to Korell et al. Glob. Chang. Biol. https://doi.org/10.1111/gcb.14854.
Duan, M., Bax, C., Laakso, K., Mashhadi, N., Mattie, N., Sanchez-Azofeifa, A., 2023. Characterizing transitions between successional stages in a tropical dry Forest using LiDAR techniques. Remote Sens. 15. https://doi.org/10.3390/rs15020479.
Duchesne, J., Raimbault, P., Fleurant, C., 2001. Towards a universal law of tree morphometry by combining fractal geometry and statistical physics. In: Emergent Nature: Patterns, Growth and Scaling in the Sciences. World Scientific, pp. 93–102. https://doi.org/10.1142/9789812777720_0008.
Edeline, E., Bennevault, Y., Rozen-Rechels, D., 2023. Habitat complexity-productivity relationships Habitat structural complexity increases age-class coexistence and productivity in fish populations. https://doi.org/10.1101/2023.07.18.549540.
Ehbrecht, M., Seidel, D., Annighöfer, P., Kreft, H., Köhler, M., Zemp, D.C., Puettmann, K., Nilus, R., Babweteera, F., Willim, K., Stiers, M., Soto, D., Boehmer, H.J., Fisichelli, N., Burnett, M., Juday, G., Stephens, S.L., Ammer, C., 2021. Global patterns and climatic controls of forest structural complexity. Nat. Commun. 12. https://doi.org/10.1038/s41467-020-20767-z.
Enquist, B.J., Niklas, K.J., 2001. Invariant scaling relations across tree-dominated communities. Nature. 410 (6829), 655–660.
Faccion, G., Alves, A.M., do Espírito-Santo, M.M., Silva, J.O., Sanchez-Azofeifa, A., Ferreira, K.F., 2021. Intra- and Interspecific Variations on Plant Functional Traits along a Successional Gradient in a Brazilian Tropical Dry Forest. Flora: Morphology, Distribution, Functional Ecology of Plants, p. 279. https://doi.org/10.1016/j.flora.2021.151815.
Fath, B.D., Jørgensen, S.E., Patten, B.C., Straškraba, M., 2004. Ecosystem growth and development. BioSystems 77, 213–228. https://doi.org/10.1016/j.biosystems.2004.06.001.
Feeley, K.J., Davies, S.J., Perez, R., Hubbell, S.P., Foster, R.B., 2011. Directional changes in the species composition of a tropical forest. Ecology 92, 871–882. https://doi.org/10.1890/10-0724.1.
Gamfeldt, L., Roger, F., 2017. Revisiting the biodiversity-ecosystem multifunctionality relationship. Nat. Ecol. Evol. https://doi.org/10.1038/s41559-017-0168.
Gandharum, L., Sadmono, H., Sencaki, D.B., Eugenie, A., Prayogi, H., Cahyaningtiyas, I. F., 2022. Application of Hyperspectral Airborne Data for Discriminating Tree Species in Tropical Peat Swamp Forest, Indonesia. In: 2022 IEEE Asia-Pacific Conference on Geoscience, Electronics and Remote Sensing Technology (AGERS), pp. 54–59.
Geary, W.L., Bode, M., Doherty, T.S., Fulton, E.A., Nimmo, D.G., Tulloch, A.I.T., Tulloch, V.J.D., Ritchie, E.G., 2020. A guide to ecosystem models and their environmental applications. Nat. Ecol. Evol. https://doi.org/10.1038/s41559-020-01298-8.
Gibbs, H.K., Brown, S., Niles, J.O., Foley, J.A., 2007. Monitoring and estimating tropical forest carbon stocks: making REDD a reality. Environ. Res. Lett. 2. https://doi.org/10.1088/1748-9326/2/4/045023.
Gini, Corrado, 1912. Studi economico-giuridici pubblicati per cura della facoltà di Giurisprudenza della R. Università di Cagliari. Tipogr. di P. Cuppini.
Gini, C., 1921. Measurement of inequality of incomes, source. Econ. J. 31 (121), 124–126. https://doi.org/10.2307/2223319.
Golden Software, 2024.
Gu, Z., Cao, S., Sanchez-Azofeifa, G.A., 2018. Using LiDAR waveform metrics to describe and identify successional stages of tropical dry forests. Int. J. Appl. Earth Obs. Geoinf. 73, 482–492. https://doi.org/10.1016/j.jag.2018.07.010.
Guariguata, M.R., Ostertag, R., 2000. Neotropical Secondary Forest Succession: Changes in Structural and Functional Characteristics.
Guariguata, M.R., Ostertag, R., 2001. Neotropical secondary forest succession: changes in structural and functional characteristics. For. Ecol. Manag. 148, 185–206. https://doi.org/10.1016/S0378-1127(00)00535-1.
Guralnick, R., Jetz, W., Meyer, C., Kreft, H., 2015. Of biodiversity distributions. Nat. Commun. 6, 1–8. https://doi.org/10.1038/ncomms9221.
Hamby, D.M., 1994. A review of techniques for parameter sensitivity analysis of environmental models. Environ. Monit. Assess. 32, 135–154.
Harte, J., Brush, M., Newman, E.A., Umemura, K., 2022. An equation of state unifies diversity, productivity, abundance and biomass. Commun Biol 5. https://doi.org/10.1038/s42003-022-03817-8.
Hartshorn, G.S., 1980. Neotropical Forest Dynamics.
Heidrich, L., Bae, S., Levick, S., Seibold, S., Weisser, W., Krzystek, P., Magdon, P., Nauss, T., Schall, P., Serebryanyk, A., Wöllauer, S., Ammer, C., Bässler, C., Doerfler, I., Fischer, M., Gossner, M.M., Heurich, M., Hothorn, T., Jung, K., Kreft, H., Schulze, E.D., Simons, N., Thorn, S., Müller, J., 2020. Heterogeneity–diversity relationships differ between and within trophic levels in temperate forests. Nat. Ecol. Evol. 4, 1204–1212. https://doi.org/10.1038/s41559-020-1245-z.
Hill, M.O., 1973. Diversity and Evenness: A Unifying Notation and Its Consequences, 54, pp. 427–432. https://doi.org/10.2307/1934352.
Hong, P., Schmid, B., De Laender, F., Eisenhauer, N., Zhang, X., Chen, H., Craven, D., De Boeck, H.J., Hautier, Y., Petchey, O.L., Reich, P.B., Steudel, B., Striebel, M., Thakur, M.P., Wang, S., 2022. Biodiversity promotes ecosystem functioning despite environmental change. Ecol. Lett. https://doi.org/10.1111/ele.13936.
Hordijk, I., Maynard, D.S., Hart, S.P., Lidong, M., Ter Steege, H., Liang, J., de Miguel, S., Nabuurs, G.-J., Reich, P.B., Abegg, M., Others, 2023. Evenness mediates the global relationship between forest productivity and richness. J. Ecol. 111, 1308–1326.
Huxley, J.D., White, C.T., Humphries, H.C., Weber, S.E., Spasojevic, M.J., 2023. Plant functional traits are dynamic predictors of ecosystem functioning in variable environments. J. Ecol. 111, 2597–2613.
Janzen, D.H., 1988. Management of Habitat Fragments in a Tropical Dry Forest: Growth, Source: Annals of the Missouri Botanical Garden.
Jiménez-Rodríguez, C.D., Coenders-Gerrits, M., Wenninger, J., Gonzalez-Angarita, A., Savenije, H., 2020. Contribution of understory evaporation in a tropical wet forest during the dry season. Hydrol. Earth Syst. Sci. 24, 2179–2206. https://doi.org/10.5194/hess-24-2179-2020.
Jost, L., 2006. Entropy and diversity. OIKOS 113, 363–375. https://doi.org/10.1111/j.2006.0030-1299.14714.x.
Jost, L., 2010. The relation between evenness and diversity. Diversity (Basel) 2, 207–232. https://doi.org/10.3390/d2020207.
Kalacska, M., Sanchez-Azofeifa, G.A., Calvo-Alvarado, J.C., Quesada, M., Rivard, B., Janzen, D.H., 2004. Species composition, similarity and diversity in three successional stages of a seasonally dry tropical forest. For. Ecol. Manag. 200. https://doi.org/10.1016/j.foreco.2004.07.001.
Kalácska, M., Calvo-Alvarado, J.C., Sánchez-Azofeifa, G.A., 2005. Calibration and assessment of seasonal changes in leaf area index of a tropical dry forest in different stages of succession. Tree Physiol. 25. https://doi.org/10.1093/treephys/25.6.733.
Knight, D.H., 1975. A Phytosociological Analysis of Species-Rich Tropical Forest on Barro Colorado Island, Panama.
Kohn, A.J., Leviten, P.J., 1976. Effect of habitat complexity on population density and species richness in tropical intertidal predatory gastropod assemblages. Oecologia 25, 199–210. https://doi.org/10.1007/BF00345098.
Konopiński, M.K., 2020. Shannon diversity index: a call to replace the original Shannon's formula with unbiased estimator in the population genetics studies. PeerJ 2020. https://doi.org/10.7717/peerj.9391.
Koop, H., Rijksen, H.D., Wind, J., 1995. Tools to Diagnose Forest Integrity; an Appraisal Method Substantiated by Silvi-Star Assessment of Diversity and Forest Structure.
Kvålseth, T.O., 1991. Note on Biological Diversity, Evenness, and Homogeneity Measures.
Lawton, J.H., 1999. Are there General Laws in Ecology? Introduction and definitions, Source: Oikos. https://doi.org/10.2307/3546712.
Levene, H., 1960. Robust tests for equality of variances. Contributi. Probabili. Statist. 278–292.
Lexerød, N.L., Eid, T., 2006. An evaluation of different diameter diversity indices based on criteria related to forest management planning. For. Ecol. Manag. 222, 17–28. https://doi.org/10.1016/j.foreco.2005.10.046.
Li, H., Reynolds, J.F., 1993. A new contagion index to quantify spatial patterns of landscapes. Landsc. Ecol. 8, 155–162.
Li, J., Zhang, J., Ge, W., Liu, X., 2004. Evaluating Landsat thematic mapper spectral indices for estimating burn severity of the 2007 Peloponnese wildfires in Greece. Int. J. Wildland Fire 19, 558–569. https://doi.org/10.1016/j.ces.2004.01.025.
Liesenberg, V., 2022. Characterizing Biophysical Attributes in Tropical Secondary Forest Environments with Multitemporal Hyperspectral Images. In: IGARSS 2022–2022 IEEE International Geoscience and Remote Sensing Symposium, pp. 5656–5659.
Liu, X., Ma, Q., Wu, X., Hu, T., Liu, Z., Liu, L., Guo, Q., Su, Y., 2022. A novel entropy-based method to quantify forest canopy structural complexity from multiplatform lidar point clouds. Remote Sens. Environ. 282. https://doi.org/10.1016/j.rse.2022.113280.
Liu, C., Sanchez-Azofeifa, A., Bax, C., 2023. Studying tropical dry forests secondary succession (2005–2021) using two different LiDAR systems. Remote Sens. 15. https://doi.org/10.3390/rs15194677.
Lohbeck, M., Poorter, L., Paz, H., Pla, L., van Breugel, M., Martínez-Ramos, M., Bongers, F., 2012. Functional diversity changes during tropical forest succession. Perspect Plant Ecol. Evol. Syst. 14, 89–96. https://doi.org/10.1016/j.ppees.2011.10.002.

Lorenz, M.O., 1905. Methods of Measuring the Concentration of Wealth. Association (Vol. 9, Issue 70)..

Luo, S., Phillips, R.P., Jo, I., Fei, S., Liang, J., Schmid, B., Eisenhauer, N., 2023. Higher productivity in forests with mixed mycorrhizal strategies. Nat. Commun. 14. https://doi.org/10.1038/s41467-023-36888-0.

Macarthur, R.H., Macarthur, J.W., 1961. On Bird Species Diversity, Source: Ecology.

MacDonald, Z.G., Nielsen, S.E., Acorn, J.H., 2017. Negative relationships between species richness and evenness render common diversity indices inadequate for assessing long-term trends in butterfly diversity. Biodivers. Conserv. 26, 617–629. https://doi.org/10.1007/s10531-016-1261-0.

Madin, J.S., Asbury, M., Schiettekatte, N., Dornelas, M., Pizarro, O., Reichert, J., Torres-Pulliza, D., 2023. A word on habitat complexity. Ecol. Lett. 26, 1021–1024. https://doi.org/10.1111/ele.14208.

Magurran, Anne E., 2004. Measuring Biological Diversity. Blackwell Science, Oxford, UK.

Malhi, Y., Doughty, C.E., Goldsmith, G.R., Metcalfe, D.B., Girardin, C.A.J., Marthews, T. R., del Aguila-Pasquel, J., Aragão, L.E.O.C., Araujo-Murakami, A., Brando, P., da Costa, A.C.L., Silva-Espejo, J.E., Farfán Amézquita, F., Galbraith, D.R., Quesada, C. A., Rocha, W., Salinas-Revilla, N., Silvério, D., Meir, P., Phillips, O.L., 2015. The linkages between photosynthesis, productivity, growth and biomass in lowland Amazonian forests. Glob. Chang. Biol. 21, 2283–2295. https://doi.org/10.1111/gcb.12859.

Malhi, Y., Riutta, T., Wearn, O.R., Deere, N.J., Mitchell, S.L., Bernard, H., Majalap, N., Nilus, R., Davies, Z.G., Ewers, R.M., Struebig, M.J., 2022. Logged tropical forests have amplified and diverse ecosystem energetics. Nature 612, 707–713. https://doi.org/10.1038/s41586-022-05523-1.

Mason, N.W.H., Mouillot, D., Lee, W.G., Wilson, J.B., Setälä, H., 2005. Functional Richness, Functional Evenness and Functional Divergence: The Primary Components of Functional Diversity, Source: Oikos.

Meffe, G., Nielsen, L., Knight, R.L., Schenborn, D., 2002. Ecosystem management: adaptive. Community-Based Conservat..Island Press, Washington, DC, USA, pp. 1–333.

Meyer, V., Saatchi, S., Clark, D.B., Keller, M., Vincent, G., Ferraz, A., Espírito-Santo, F., D'Oliveira, M.V.N., Kaki, D., Chave, J., 2018. Canopy area of large trees explains aboveground biomass variations across neotropical forest landscapes. Biogeosciences 15, 3377–3390. https://doi.org/10.5194/bg-15-3377-2018.

Mitchell, J.C., Kashian, D.M., Chen, X., Cousins, S., Flaspohler, D., Gruner, D.S., Johnson, J.S., Surasinghe, T.D., Zambrano, J., Buma, B., 2023. Forest ecosystem properties emerge from interactions of structure and disturbance. Front. Ecol. Environ. 21, 14–23. https://doi.org/10.1002/fee.2589.

Moreno, S.O., Gentleman, R., Ihaka, R., Ripley, B., Maechler, M., Murdoch, Duncan, 2023. Savitzky-Golay filtering for R. Anal. Chem. https://doi.org/10.1021/ac60214a047.

Morris, E.K., Caruso, T., Buscot, F., Fischer, M., Hancock, C., Maier, T.S., Meiners, T., Müller, C., Obermaier, E., Prati, D., Socher, S.A., Sonnemann, I., Wäschke, N., Wubet, T., Wurst, S., Rillig, M.C., 2014. Choosing and using diversity indices: insights for ecological applications from the German biodiversity Exploratories. Ecol. Evol. 4, 3514–3524. https://doi.org/10.1002/ece3.1155.

Muss, J.D., Aguilar-Amuchastegui, N., Mladenoff, D.J., Henebry, G.M., 2013. Analysis of waveform lidar data using shape-based metrics. IEEE Geosci. Remote Sens. Lett. 10, 106–110. https://doi.org/10.1109/LGRS.2012.2194472.

Neumann, M., Starlinger, F., 2001. The Signi®Cance of Different Indices for Stand Structure and Diversity in Forests.

Newsome, A.E., Catling, P.C., 1979. Habitat preferences of mammals inhabiting heathlands of warm temperate coastal, montane and alpine regions of southeastern Australia. Ecosyst. World 9.

Nielsen, S.N., Müller, F., Marques, J.C., Bastianoni, S., Jørgensen, S.E., 2020. Thermodynamics in ecology-an introductory review. Entropy. https://doi.org/10.3390/E22080820.

Orlóci, L., 1991. Entropy and Information. Lecture notes in Statistical Biology View project Outlier identification View Project.

Papastefanou, P., Esquivel-Muelbert, A., Suvanto, S., Olin, S., Crowther, T., Schelhaas, M.-J., Pugh, T., 2023. Improving ecosystem model development with machine learning: a full hybrid approach. In: EGU General Assembly Conference Abstracts. EGU–9948.

Parkes, D., Newell, G., Cheal, D., 2003. Assessing the Quality of Native Vegetation: The "Habitat Hectares" Approach.

Petrokas, R., 2020. Forest climax phenomenon: an invariance of scale. Forests. https://doi.org/10.3390/f11010056.

Poorter, L., Bongers, F., Aide, T.M., Almeyda Zambrano, A.M., Balvanera, P., Becknell, J. M., Boukili, V., Brancalion, P.H.S., Broadbent, E.N., Chazdon, R.L., Craven, D., De Almeida-Cortez, J.S., Cabral, G.A.L., De Jong, B.H.J., Denslow, J.S., Dent, D.H., DeWalt, S.J., Dupuy, J.M., Durán, S.M., Espírito-Santo, M.M., Fandino, M.C., César, R.G., Hall, J.S., Hernandez-Stefanoni, J.L., Jakovac, C.C., Junqueira, A.B., Kennard, D., Letcher, S.G., Licona, J.C., Lohbeck, M., Marín-Spiotta, E., Martínez-Ramos, M., Massoca, P., Meave, J.A., Mesquita, R., Mora, F., Munõz, R., Muscarella, R., Nunes, Y.R.F., Ochoa-Gaona, S., De Oliveira, A.A., Orihuela-Belmonte, E., Penã-Claros, M., Pérez-Garciá, E.A., Piotto, D., Powers, J.S., Rodríguez-Velázquez, J., Romero-Pérez, I.E., Ruíz, J., Saldarriaga, J.G., Sanchez-Azofeifa, A., Schwartz, N.B., Steininger, M.K., Swenson, N.G., Toledo, M., Uriarte, M., Van Breugel, M., Van Der Wal, H., Veloso, M.D.M., Vester, H.F.M., Vicentini, A., Vieira, I. C.G., Bentos, T.V., Williamson, G.B., Rozendaal, D.M.A., 2016. Biomass resilience of Neotropical secondary forests. Nature 530, 211–214. https://doi.org/10.1038/nature16512.

Pos, E., de Souza Coelho, L., de Andrade Lima Filho, D., Salomão, R.P., Amaral, I.L., de Almeida Matos, F.D., Castilho, C.V., Phillips, O.L., Guevara, J.E., de Jesus Veiga Carim, M., Others, 2023. Unraveling Amazon tree community assembly using maximum information entropy: a quantitative analysis of tropical forest ecology. Sci. Rep. 13, 2859.

Ray, T., Delory, B.M., Beugnon, R., Bruelheide, H., Cesarz, S., Eisenhauer, N., Ferlian, O., Quosh, J., von Oheimb, G., Fichtner, A., 2023. Tree diversity increases productivity through enhancing structural complexity across mycorrhizal types. Sci. Adv. 9, eadi2362.

Roswell, M., Dushoff, J., Winfree, R., 2021. A conceptual guide to measuring species diversity. Oikos 130, 321–338. https://doi.org/10.1111/oik.07202.

Rozendaal, A., Bongers, D.M., Aide, F. Mitchell, Alvarez-Dávila, T., Ascarrunz, E., Balvanera, N., Becknell, P., Bentos, J.M., Brancalion, T.V.S., Cabral, P.H.L., Calvo-Rodriguez, G.A., Chave, S., César, J., Espírito-Santo, R.G., Fandino, M.M., Fernandes, M.C. Wilson, Finegan, G., García, B., Gonzalez, H., Moser, N. Granda, Hall, V., Hernández-Stefanoni, J.S. Luis, Hubbell, J., Jakovac, S., Hernández, C.C. Johanna, Junqueira, A., Kennard, A.B., Larpin, D., Letcher, D., Licona, S.G., Lebrija-Trejos, J.-C., Marín-Spiotta, E., Martínez-Ramos, E., Massoca, M.S., Meave, P.E., Mesquita, J.A.G., Mora, R.C., Müller, F., Muñoz, S.C., de Oliveira Neto, R. Nolasco, Norden, S., Nunes, N.F., Ochoa-Gaona, Y.R., Ortiz-Malavassi, S., Ostertag, E., Peña-Claros, R., Pérez-García, M., Piotto, E.A., Powers, D., Aguilar-Cano, J.S., Rodriguez-Buritica, J., Rodríguez-Velázquez, S., Romero-Romero, J. Antonio, Ruíz, M., Sanchez-Azofeifa, J., de Almeida, A. Silva, Silver, A., Schwartz, W.L., Thomas, N.B. Wayt, Toledo, W., Uriarte, M., de Sá Sampaio, M. Valadares, van Breugel, E., van der Wal, M., Martins, H. Venâncio, Veloso, S.M., Vester, M.D.M., Vicentini, H.F., Vieira, A.G., Villa, I.C., Williamson, P. Bruce, Zanini, G., Zimmerman, K.J., Poorter, J.L., 2019. Biodiversity Recovery of Neotropical Secondary Forests. Saara J, DeWalt.

Saltelli, A., Tarantola, S., Campolongo, F., 2000. Sensitivity analysis as an ingredient of modeling. Stat. Sci. 377–395.

Schnabel, F., Schwarz, J.A., Dănescu, A., Fichtner, A., Nock, C.A., Bauhus, J., Potvin, C., 2019. Drivers of productivity and its temporal stability in a tropical tree diversity experiment. Glob. Chang. Biol. 25, 4257–4272. https://doi.org/10.1111/gcb.14792.

Shannon, C.E., 1948. A mathematical theory of communication. Bell Syst. Tech. J. https://doi.org/10.1002/j.1538-7305.1948.tb01338.x.

Sitthiyot, T., Holasut, K., 2021. A simple method for estimating the Lorenz curve. Humanit Soc Sci Commun 8. https://doi.org/10.1057/s41599-021-00948-x.

Spies, T.A., Franklin, J.F., 1991. The Structure of Natural Young, Mature, and Old-Growth Douglas-Fir Forests in Oregon and Washington.

St. Pierre, J.I., Kovalenko, K.E., 2014. Effect of habitat complexity attributes on species richness. Ecosphere 5. https://doi.org/10.1890/ES13-00323.1.

Stirling, G., Wilsey, B., 2001. Empirical relationships between species richness, evenness, and proportional diversity. Am. Nat. 158, 286–299. https://doi.org/10.1086/321317.

Svirezhev, Y.M., 2000. Thermodynamics and ecology. Ecol 132 (1–2), 11–22.

Tilman, D., Isbell, F., Cowles, J.M., 2014. Biodiversity and ecosystem functioning. Annu. Rev. Ecol. Evol. Syst. 45, 471–493. https://doi.org/10.1146/annurev-ecolsys-120213-091917.

Tuomisto, Hanna, Tuomisto, H., 2012. An updated consumer's guide to evenness and related indices. https://doi.org/10.1111/j.16000706.2011.19897.x.

Valbuena, R., Nabuurs, G.-J., 2013. Patterns of covariance between airborne laser scanning metrics and Lorenz curve descriptors of tree size inequality, Joensuu, Finland. Can. J. Remote. Sens., 39(sup1), S18-S31.

Valbuena, R., Packalén, P., Martín-Fernández, S., Maltamo, M., 2012. Diversity and equitability ordering profiles applied to study forest structure. For. Ecol. Manag. 276, 185–195. https://doi.org/10.1016/j.foreco.2012.03.036.

Valbuena, R., Packalen, P., Mehtätalo, L., García-Abril, A., Maltamo, M., 2013. Characterizing forest structural types and shelterwood dynamics from Lorenz-based indicators predicted by airborne laser scanning. Can. J. For. Res. 43, 1063–1074. https://doi.org/10.1139/cjfr-2013-0147.

Valbuena, R., Eerikäinen, K., Packalen, P., Maltamo, M., 2016. Gini coefficient predictions from airborne lidar remote sensing display the effect of management intensity on forest structure. Ecol. Indic. 60, 574–585. https://doi.org/10.1016/j.ecolind.2015.08.001.

Valbuena, R., Adnan, S., Maltamo, M., Mehtätalo, L., Ammaturo, R.N.L., Lovejoy, T., 2021. Moving on from foliage height diversity: determining maximum entropy in 3-dimensional variables. https://doi.org/10.34726/wim.1861.

Van, D., Meerssehaut, D., Vandekerkhove, K., 2000. Development of a Stand-Scale Forest Biodiversity Index Based on the State Forest Inventory.

Vranken, I., Baudry, J., Aubinet, M., Visser, M., Bogaert, J., 2015. A review on the use of entropy in landscape ecology: heterogeneity, unpredictability, scale dependence and their links with thermodynamics. Landsc. Ecol. https://doi.org/10.1007/s10980-014-0105-0.

Wang, C., Zhao, H., 2018. Spatial heterogeneity analysis: introducing a new form of spatial entropy. Entropy 20. https://doi.org/10.3390/e20060398.

Weiner, J., Solbrig, O.T., 1984. The meaning and measurement of size hierarchies in plant populations. Oecologia 61. https://doi.org/10.1007/BF00379630.

Weiner, J., Mcclure, M.S., Hastings, A., Horn, C.L., Brougham, R.W., Harris, W., Simms, E.L., Rausher, M.M.D., Witte, L., Wippich, C., Wink, M.R., Biehl, B., Ciesemann, A., Zangerl, M.R.A.R., Nitao, I.K., Bosque-Perez, N.A., Foster, K.W., Leigh, T.F., Matzinger, D.F., Wernsman, E.A., Weeks, W.W., Eikenbary, R.D.D.J., 1990. Asymmetric competition in plant populations. Trends Ecol. Evol. 5, 360–364.

Wright Muelas, M., Mughal, F., O'Hagan, S., Day, P.J., Kell, D.B., 2019. The role and robustness of the Gini coefficient as an unbiased tool for the selection of Gini genes for normalising expression profiling data. Sci. Rep. 9. https://doi.org/10.1038/s41598-019-54288-7.

Xu, C., Hu, Y., Chang, Y., Jiang, Y., Li, X., Bu, R., He, H., 2004. Sensitivity analysis in ecological modeling. Ying Yong Sheng Tai Xue Bao 15, 1056–1062.

Yan, P., He, N., Yu, K., Xu, L., Van Meerbeek, K., 2023a. Integrating multiple plant functional traits to predict ecosystem productivity. Commun Biol 6, 239.

Yan, H., Li, F., Liu, G., 2023b. Diminishing influence of negative relationship between species richness and evenness on the modeling of grassland α-diversity metrics. Front. Ecol. Evol. 11. https://doi.org/10.3389/fevo.2023.1108739.

Zaccarelli, N., Li, B.L., Petrosillo, I., Zurlini, G., 2013. Order and disorder in ecological time-series: introducing normalized spectral entropy. Ecol. Indic. 28, 22–30. https://doi.org/10.1016/j.ecolind.2011.07.008.

Zenner, E.K., 2000. Do residual trees increase structural complexity in Pacific northwest coniferous forests? Ecol 10 (3), 800–810.

Zhao, G., Sanchez-Azofeifa, A., Laakso, K., Sun, C., Fei, L., 2021. Hyperspectral and full-waveform lidar improve mapping of tropical dry forest's successional stages. Remote Sens. 13. https://doi.org/10.3390/rs13193830.

Valbuena, R., 2015. Forest structure indicators based on tree size inequality and their relationships to airborne laser scanning. Dissertationes Forestales, 2015. 10.14214/df.205.